SAMPLING OR INTERMITTENCY IN HAND CONTROL SYSTEM DYNAMICS

FERNANDO NAVAS *and* LAWRENCE STARK

From the Neurology Section, Massachusetts Institute of Technology, Cambridge, Massachusetts 02139. Dr. Stark's present address is Presbyterian-St. Lukes' Hospital, College of Engineering, University of Illinois, Chicago, Illinois 60680. Dr. Navas' present address is the University of Los Andes, Bogota, Colombia.

ABSTRACT A hand control model is proposed. Investigation of the hand's intermittency synchronization shows it corresponds to an input-synchronized sampler rather than the clock-synchronized sampler more typical of engineering systems. A velocity control mechanism, similar to that in an eye tracking system is shown to be absent in the hand. A quantitative transfer function for predictable inputs serves further to define the hand's input adaptive characteristics. Stability margin adjustments of a linear reduced model enabled us to match the available quantitative data. The most exciting result of this study is the evidence for intermittency: a refractory period shown in the short pulse experiment, peaks in the frequency response experiments, and a saccadic sequence of steps in response to an open loop step input and to a closed loop ramp input.

INTRODUCTION

We have examined the control system for human hand movement, using the approaches of several different disciplines. In studying the performance of the system, its limits, and possibilities from the viewpoint of a human engineer, we have used a tracking situation and complex inputs to obtain a variety of frequency responses. We have utilized known facts and data from the physiological literature, and have also simulated muscle and muscle spindle dynamics to define the blocks within the total motor control system of man (13). As neurologists, we have organized the "topology" of these physiological elemental blocks into a model in a manner that seems compatible with actual neurological organization as far as this is known. To further refine and assess our model, we have utilized studies in persons with neurological defects such as Parkinson's disease, and have studied the effects of drugs producing temporary paralysis of gamma efferent fibers. Finally, as control engineers interested in neurological control systems, we have used special experimental techniques such as opening loops by clamping methods in order to expose certain essential characteristics of this feedback control system.

Some of the characteristic features of our model, which we present and describe, have been derived from physiological information, some from our experimental results, and some remain untested assumptions. Ward (20), Bekey (1), Lemay and Westcott (8) have postulated sampled data models for the hand, Smith and Cortes (2, 12) a "bang-bang" system. Psychologists since Telford (18) have been interested in psychological refractory period and intermittency in voluntary responses. Russell and Tustin (19) and Elkind (4) have defined frequency characteristics of manual control. And work has been done by our group (at the Neurology Section of the Massachusetts Institute of Technology, now at University of Illinois, Chicago Circle) defining physiological elements and neurological organization, studying experimentally and by simulation transient and steady-state behavior (14), and sampled data characteristics of hand and eye tracking systems (11).

After a description of the equipment, the experimental section describes results for four types of inputs: closed loop transients, open loop and variable feedback transients, closed loop continuous unpredictable signals, and predictable signals.

In the discussion section we evaluate our model and relate our work to previously published research in this field as well as to other models. The evidence for intermittency in the hand control system is developed in full during an expanded discussion of the various experiments, observations, and assumptions of our studies.

In the conclusion we attempt to summarize the present status of our knowledge of the human control system for hand movement.

THE MODEL

Sampled Data Characteristics

Recent studies have suggested that the eye movement tracking system can be treated as a sampled data system (21, 22) since the discrete nature of sampled data systems is in some sense similar to the notion of a refractory period, a common phenomenon in neurophysiology. Other discontinuous control systems such as quantized systems have properties in common with sampled data systems, and indeed the hand movement system demonstrates characteristics of quantization as well (15).

When slowly moving ramps are used as input target signals, and the subject is tracking this input with a device that offers very small mechanical impedance, a response similar to the one shown in Fig. 1 is seen. The output response consists of step-like changes in position which occur at irregular intervals and amplitudes. The output signal rotary motion transducer had an effectively infinite resolution, and neither friction nor any other component of the mechanical impedance of the transducer was of sufficient magnitude to play an important role in the dynamics of the system.

When pulses of varying width are used as input target signals and are presented irregularly in time, a response that is similar to that shown in Fig. 2 *a* is obtained.

There are delays of approximately 150–250 msec before the rapid response motions occur for both leading and trailing edges of the input target motion. This delay in response has several components in addition to nerve conduction time and is sometimes called the "psychological refractory period" (18).

When a pulse of extremely narrow width is supplied unpredictably as an input target motion, a normal delay occurs before the response movement to the leading edge of the input motion as Fig. 2 *b* illustrates. However, the response movement to the trailing edge of the input motion has a much more prolonged delay, 400 msec, as in the case illustrated in Fig. 2 *b*. This prolonged delay can be accounted for as a normal refractory period that starts after the initial response motion, rather than being triggered by the trailing edge of the input target. This behavior would be characteristic of a sampled data system.

For a motor coordination sampled data system with the transient responses shown in Figs. 1 and 2, the frequency response to wide bandwidth inputs could demonstrate a peak at one-half the sampling frequency, or at approximately 2 cps, as well as an absence of coherent tracking characteristics at frequencies greater than this peaking frequency. There exists very little experimental data that clearly support the occurrence of this suggested peaking frequency since most of the experiments have used input spectra with either lower frequencies than 2 cps or else too little power at higher frequencies to obtain effective responses necessary to demonstrate the peak. Bekey (1), in the most complete study of sampled data properties of the manual tracking control system, was able to show peaking at half sampling frequencies only in spectral curves of error. However, Stark, Iida, and Willis (14) have described frequency response experiments that were not limited by these undesirable input spectrum characteristics. The clearly defined peak in the response spectrum in Fig. 3 supports the idea that the human motor coordination system can be treated as a sampled data control system.

The adequacy of representing the hand movement system as a feedback control system has been shown by various human engineering investigators (4, 7, 9, 10, 19). Furthermore, on the basis of our own experimental results such as short pulse (Fig. 2) and the ramp responses shown in Fig. 4 (reference 15), as well as the findings of others (1, 6, 20), we decided that some kind of intermittency should be included.

For unpredictable inputs, the human tracking system acts as a position feedback control system with important discontinuous properties in the frequency range of interest. Its intermittency is related to an interesting alternation of control of the muscles by ballistic voluntary inputs and by a stabilizing proprioceptive reflex loop. The actuating signal of the system includes a combination of error and input (pursuit tracking) which compensates for some of the inherent delays. For predictable inputs, different continuous models which include ideal predictors are applicable. The model to be presented has a number of characteristic features, each of which will be discussed in detail, justified by experiment where possible, and related in the discussion to results in the literature.

The Model

The model for pursuit tracking of unpredictable inputs is presented in Fig. 5 *a* in block diagrammatic form. Note: (*a*) the visual feedback path and the integrator in the loop which makes the system a position servo; (*b*) the additional proprioceptive feedback path; (*c*) the switch providing an intermittency or quasi-sampled data action; (*d*) the alternation between voluntary and reflex action for control; and (*e*) the observation of the input which allows for some delay compensation through the lead term $(1 + k_2 s/k_1)$.

This block diagram necessarily includes elements from the visual, central nervous, and muscular systems.

EXPERIMENTAL METHOD

The experimental arrangement, shown in Fig. 6, includes the "light-coordination machine" and peripheral equipment for the analysis and generation of signals. Certain modifications were made in the apparatus in order to adapt it for rapid transient visual inputs, and to permit mechanical impulses to be injected (13).

The light-coordination machine consists of a linear mirror galvanometer which transforms an electric signal into a display of a light pencil, a screen, a pointer, and an angular potentiometer as the mechanical-to-electrical transducer. The subject tried to follow and reproduce the display by rotation of his wrist. The response of the subject (rotation of the wrist) was measured by a precision continuous (infinite resolution) potentiometer, and, in addition to this angle θ_o, we could obtain $\dot{\theta}_o$ and $\ddot{\theta}_o$ by differentiating.

The handle of the machine was very light and had negligible friction. When no extra load was added, it acted as a small inertia load on the arm. Accelerations as high as 400°/sec² were recorded. The apparatus required very small forces, much less than 100 *g*. This was a favorable feature since the apparent viscosity of the muscle increases with the degree of activation.

The method of studying the rotation of the wrist of an awake cooperative subject has been described in an earlier paper where impulses, pulses, and steps, all with unpredictable times of occurrence, were contrasted with successions of regular square waves of target position in addition to single sinusoids, and sums of incommensurate sinusoids, the pseudorandom signal previously described (14).

Peripheral equipment of the experimental arrangement included function generators, filters, operational amplifier set for signal transformation, recorders, measuring equipment, a pendulum for application of mechanical impulses, and a computer with digital-to-analog and analog-to-digital conversion equipment. The computer was used for the frequency domain characterization of the human operator using programs developed by our group in the Neurology Section of the Electronic Systems Laboratory at the Massachusetts Institute of Technology. The computer produced a combination of sinusoids of arbitrary magnitude and phase, and it made a Fourier analysis of the operator's response to these signals.

Eye-Hand Comparisons

Because of the large variation in response of both the hand and the eye systems with different subjects, with minor modifications of the experimental apparatus, and with time, we decided to measure both of these systems' responses simultaneously (15, 16).

The eye muscles have considerable power with respect to their constant load, the eyeball, and show faster rise times than the hand, especially when tracking rapidly alternating signals

as shown in Fig. 7 *c*. Examples of eye and hand responses to irregular steps and slower regular steps were recorded simultaneously and are illustrated in Fig. 7; for these inputs the eye has shorter response times than the hand.

At moderate frequencies (0.7–1.0 cps) the hand develops prediction faster and to a greater extent than the eye. At higher frequencies (1.2 cps) the hand shows considerable prediction, while the median eye response time starts to lag in spite of the higher frequency characteristics of the actual movement dynamics of the eye. At low frequencies, there is some correlation evident between eye and hand response times as is shown in Fig. 7.

EXPERIMENTAL RESULTS

Closed Loop Transients (Unpredictable Inputs)

Closed loop transients included visual pulses and approximations to impulses, mechanical impulses, visual steps, and ramps. Examples of typical performances are presented.

Input Pulses. Responses to input pulses are shown in Fig. 8. For unpredictable short pulses there were intervals from 0.15–0.30 sec between the two halves of the response, as can be seen from Figs. 8 *c* and 8 *d*. This was no longer true for predictable short pulses shown in Fig. 8 *e*. Notice also the fairly consistent overshoots in the initial correction, the oscillatory hunting, and the decrease of velocity after the proper output level is achieved. The addition of moderate load seems to decrease the natural frequency and the acceleration of the arm.

Figs. 9 and 10 show the responses to visual and mechanical impulses (13). The visual impulse was a very narrow light pulse of more than 20°, and the mechanical impulse was a disturbance applied to the pointer axis by means of the pendulum. It is of interest to fit these "impulse responses" to a simple model, a second order system, which thus characterizes the motor end of the control system. The mechanical impulse response looks like a second order system; the natural frequency for the relaxed subject is 3 cps and the damping ratio is 0.15; for the tense subject the natural frequency is 5 cps and the damping ratio is 0.20. The visual impulse response is characterized by two high gain corrections, and a subsequent part representing an oscillatory decay. The first part of the response looks like an on-off action. After the first correction the situation can hardly be called unpredictable.

Input Steps. The responses of the hand control system to unpredictable steps have most of the characteristics already noted for pulse responses, and a few others. Fig. 11 shows the main types of responses, whose delay varies between 200 and 450 msec. Overshoot in the initial correction is usual, and is followed by oscillations (6–8 cps). The possibility of two-mode action is clearly seen in Figs. 11 *b*, *c*, *e*, and *f*. Fig. 12 shows the output and its velocity and acceleration for unpredictable and predictable steps. The velocity graphs consist of a triangle followed by decaying oscillations, which for the predictable case (Fig. 12 *e*), are of minor importance.

The acceleration consists of a pulse which carries the arm to the desired position followed by several alternating pulses during a braking or clamping period. For the

predictable case there is no overshoot, and the first acceleration pulse is followed by a deceleration pulse before reaching the desired position, thus suggesting a different action; small acceleration oscillations follow.

Studies of reaction time distribution for step responses have been done by Stark et al. (15, 16) as shown in Fig. 13.

Ramps. We gave considerable attention to the response of the operator to ramp inputs since the sampling or quantization limitations of the hand control system can be determined by testing with a ramp input if the system acts as a position servo. No physiological basis for a velocity servo was known; however, we were also interested in finding conditions under which the hand could exhibit velocity servo characteristics. The ramp was presented as part of a more complex combination to avoid prediction. Figs. 1, 4, 14, and 15 show inputs and responses to ramps ranging from 1.5° to 25° per sec. Figs. 16 and 17 also present velocities and accelerations. The main observation that can be derived from ramp experiments is evidence for sampling-like intermittency. Quantization or dead zone features are unimportant except for very slow ramps, less than 1° per sec. Other observations include performance deterioration for fast inputs (see Fig. 14*f*), apparently no velocity servo, and very little interpolation between samples, except possibly for some high speed inputs.

Fig. 18 shows the rise velocity of the "saccades" as a quasi-linear function of input ramp velocity. Although rise velocity changes with input velocity, this does not correspond to a velocity servo. Rather, saccadic rise velocity is more likely a function of saccadic amplitude. Figs. 19 *a* and 19 *b*, also derived from ramp responses, show that the size of the saccades is fairly linear with input velocity, and the rate of repetition of saccades is 2.5 cps for most of the input velocity range.

Observation of velocity and acceleration waveforms for ramp responses show that the series of saccades is like a collection of step responses. Fig. 20 illustrates the variation of these saccades from tense to relaxed conditions. Finally, Fig. 21 shows responses to predictable ramps for contrast.

Open Loop and Variable Feedback Transients

Open loop experiments are very useful for the analysis of biological servosystems since the models of these systems are not unique and an open loop measurement can show the order of the system and its low frequency behavior more clearly than a closed loop measurement. Variable feedback serves to correlate open loop and closed loop experiments.

Figs. 6 and 5 *b* illustrate the experimental method for open loop and variable feedback transients. The display becomes:

$$\theta_d = \theta_i + G\theta_o \tag{1}$$

where θ_i = input, and θ_o = hand output. For open loop $G = 1$, and for variable

feedback $0 < G < 1$. The error becomes:

$$\theta_e = \theta_d - \theta_o = \frac{G - 1}{G}\theta_d + \frac{1}{G}\theta_i \tag{2}$$

Short pulses and steps rather than ramps were the main inputs considered. Fig. 22 shows the responses to 100 and 200 msec pulses. From these experiments we observed that (*a*) the responses were entirely analogous to closed loop step responses; (*b*) the initial corrections were larger than but proportional to pulse size; and (*c*) the final values were related more to pulse area, and were attained after oscillations of the same frequency as in the close loop responses.

The step responses, shown in Fig. 23 look like a staircase made of saccades at a rate of 4–5 per sec. The ratio of correction to step size is again larger than unity.

Fig. 24 is an interesting correlate of these observations. The inputs are repetitive 5 and 2 cps positive pulses. The integral of this waveform appears as a ramp to a 3 cps sampler and the response looks like both the open loop step response and the closed loop ramp response.

Observations about variable feedback responses, shown in Fig. 25 are included in the discussion.

Continuous Random Inputs

As explained above, the approximations to continuous random inputs were combinations of 5–10 harmonically unrelated sinusoids generated and analyzed by a computer. Short runs (20 sec) were used to avoid operator adjustments shown by previous investigators (4, 14, 19) to depend on input spectrum.

Figs. 26 and 27 show various input spectra and the pertinent averages of gain and phase frequency response. Of the three different frequency responses, that of Fig. 27 is of the most interest, probably due to the inclusion of high frequencies. Important characteristics are: peaks in gain and related phenomena in phase around 1.5 cps; decrease in response at high frequencies which can be fitted by a -20 decilog/decade line; increase in gain from 0.5 cps up; and low frequency gain equal or less than unity.

Response to Predictable Inputs

In order to obtain a description of performance as a function of frequency, the subjects were asked to track single sinusoids. Magnitude and phase were obtained up to 3 cps. (The subjects then began to act as independent generators.) The experimental points and a fit by transfer function are shown in Fig. 28. For this fit to agree with the phase points, an ideal predictor e^{Ts} has to be included, an expected phenomenon for these predictable inputs. The transfer function was:

$$F(s) = \frac{e^{0.1s}}{(1 + 0.13s)(1 + 0.053s)(1 + 0.16s + 0.0028s^2)} \tag{3}$$

Figs. 8 *e* and 12 *e* refer also to predictable inputs, in the time domain. Fig. 21 shows the response to known triangular waves; saccades are absent and only 10 cps fluctuations show up. All these phenomena will be considered in the discussion.

DISCUSSION

Features of Model

In this section we will discuss some of the characteristic features of our model, evaluate the model itself, and relate our work to previously published research in this field as well as to other models.

Feedback System. Human engineering investigators like Tustin (19), Elkind (4), McRuer and Krendel (7, 10) have proposed feedback systems for the hand control. The human operator can apply several criteria to his tracking such as minimization of disturbance or exact reproduction of the input.

Position Servo. We can explain the topology of the model in terms of the behavior characteristics of the human operator for unpredictable inputs. That the hand system is essentially a position servo is supported by the following arguments:

(*a*) The final value of the error is zero for any kind of step input. This requires an integrator in the loop so that if a step (K/s) is applied:

$$\text{Final value} = \lim_{s \to 0} \frac{sK}{s} \frac{1}{1 + \dfrac{H(s)}{s}} = \lim_{s \to 0} \frac{Ks}{s + H(s)} = 0 \tag{4}$$

(*b*) The open loop responses shown in Figs. 22–24 give evidence of the integrator since a step input produces a (discrete) ramp, and pulse input produces a step output. A discrete ramp results also from fast repetitive steps whose integral, and that of steps half as large are equal, except for a small ripple.

(*c*) The ramp experiments show the inability of the subject to follow the input when the ramp was unpredictable; the error did not go to zero. The ramp input (v/s^2) is precisely one order higher than the tracking system.

Velocity Servo. Velocity servo characteristics are not apparent since very little interpolation appears between saccades, for ramp inputs (Figs. 1 and 14–17), and constant velocity sections are infrequent. In addition, very few corrections occur in the direction opposite to that of target when following combinations of ramps. A combination of positions and velocity servo could originate such corrections, as happens in the eye tracking system (17, 21). Of striking interest is the inability of the hand servo to smoothly follow an unpredictable ramp. The quasi-linear dependence of θ_{rise} on θ_{in} (Fig. 18) should not be confused with the action of a velocity servo.

Other Features. We will now consider other features of our model, and review previous models. Fig. 29 presents references for the discussion of compensatory and pursuit tracking configurations, as well as the models proposed by Bekey (1) and Lemay and Westcott (8) for compensatory tracking, and by Young and

Stark (17, 21) for eye tracking. Smith and Cortes (2, 12) proposed an optimal bang-bang system.

In compensatory tracking, the error is the only information received by the human being; conversely, while in pursuit tracking, both input and output are perceived (Fig. 29). Since the system is a position control system, thus requiring an integration in the loop, we choose the ideal linear pursuit model shown in Fig. 29 as a starting point. In such a model, the actuating signal is:

$$m(t) = \theta_{act} = k_2\theta_i + k_1 \int \theta_e \, dt \tag{5}$$

and

$$e'(t) = \theta_e' = \frac{1}{k_1}\frac{dm}{dt} \tag{6}$$

We attribute the operation k_1/s and a delay, T_{d2}, to the central nervous system (see Fig. 5 *a*). Although a more complex model including intermittency could be assumed for the delay and dynamics block, we try to use the simplest models for the less known parts of the tracking system; indeed, the integration in the central nervous system must be discrete in some unknown way. We attribute the delay T_{d1} to perception. The dead zone results from the experimentally verified impossibility of correcting extremely small errors.

The integrator followed by an intermittent element introduces a delay, approximately equal to $T_s/2$ where T_s is the "sampling" period. Taking this and known physiological factors into account, we divide the total response delay as follows:

Visual latencies = T_{d1}	= 40 msec
Central nervous system and AMNC intermittency = $T_s/2$ (implicit)	= 165 msec
Conduction time = T_{d2}	= 15 msec
Muscular contraction time = T_{d3}	= 30 msec
Total	= 250 msec

The dead zone varies with the individual and with the system. It may have influenced the results for very slow ramps (see Figs. 19 *a* and 19 *b*).

Tustin (19) and Elkind (4) obtained fits of the form

$$G(s) = \frac{K_c e^{-0.18s}}{1 + 0.85s} \tag{6 a}$$

for the human operator in compensatory tracking. These were optimum fits in a mean square sense, and this factor and the problem of spectrum selection may explain the absence of the integrator (9). Bekey took Elkind's fits and added sampler

and hold elements. His compensatory model thus explains the occasional peaks in the frequency response but does not explain the overshoot in the step response, the open loop and variable feedback responses, and the consistent oscillations in the transient responses except for improbable dead time resonances.

Variable Feedback Experiments

We can consider now our variable feedback experiments, ignoring intermittency since, from experimental data, it appears only to add a ripple to most outputs. We will take into account the effects of delay and hand dynamics after obtaining equations which neglect these factors (see Fig. 5 *b*):

$$\theta_d(s) = \theta_i(s) + G\theta_o(s) \tag{7}$$

$$\theta_e(s) = \theta_d(s) - \theta_o(s) \tag{8}$$

$$\theta_o(s) = k_2\theta_d(s) - \frac{k_1}{s}\theta_e(s) \tag{9}$$

solving:

$$\frac{\theta_o}{\theta_{1i}}(s) = \frac{1}{1-G}\,\frac{(1 + s^{k_2}/k_1)}{\left[1 + s\left(\frac{1 - k_2G}{(1-G)k_1}\right)\right]} \tag{10}$$

If $G = 1$,

$$\frac{\theta_o}{\theta_i}(s) = \frac{k_1}{s(1-k_2)}\left(1 + s\,\frac{k_2}{k_1}\right) \tag{11}$$

If $k_2 = 0$, but $G \neq 1$,

$$\frac{\theta_o}{\theta_i}(s) = \frac{k_1}{k_1(1-G) + s} \tag{12}$$

If $k_2 = 0$, and $G = 1$,

$$\frac{\theta_o}{\theta_i}(s) = k_1/s \tag{13}$$

If we consider Equation 13, the open loop impulse response is a delayed step with a rise time determined by hand dynamics. The step response is approximately a delayed ramp. We deduce from Equation 12 or 10 that the effect of nonunity external feedback is that the step response goes to a final value $1/(1-G)$, and the impulse response dies out fast for small G and very slowly as G approaches unity.

If we look at Equations 10 and 11, we see that the effect of k_2 is to increase initial values by correcting delays, and to increase final values by $1/(1 - k_2)$.

If $G < 1$ and $k_2 > 0$, we can expect step responses to have an initial jump of the order of $k_2/(1 - k_2G)$ and a higher final value $1/(1 - G)$. The short pulse response should die out at a high rate if G is small. Open loop experiments show that the size of the correction is generally larger than the size of the step; this observation agrees with our assumption of $k_2 \neq 0$ in Equation 5.

Variable feedback experiments shown in Fig. 25, illustrate that for pulse inputs the initial jump is independent of G, as was to be expected, and the decay rate is slightly faster for $G = \frac{1}{2}$ than for $G = \frac{2}{3}$, as expected. For step inputs the final value is higher than the initial value, and higher for $G = \frac{2}{3}$, than for $G = \frac{1}{2}$, although not as high as expected.

Prediction Operator

We recall the importance of the distinction between unpredictable and predictable tracking (13, 17):

(*a*) Comparison of Figs. 26 and 27 with Fig. 28 shows, both in magnitude and phase, the greater ability of the subject to track continuous predictable signals. Furthermore, no peaking occurs near 1.5 cps.

(*b*) Fig. 21 shows that if ramps are predictable the subject can follow them without 3 cps intermittency and with apparent velocity servo characteristics.

(*c*) Figs. 8 and 12 show clear improvement in the subject's performance when the step and pulse inputs are known beforehand.

(*d*) Response times are reduced for predictable steps (16) (Fig. 13).

(*e*) The hand system can perform very rapid and complex voluntary tasks, while it cannot follow simple unknown signals of frequencies higher than 3 or 4 cps.

When the signal is not entirely unpredictable, a whole range of intermediate situations can occur. The importance of considering unpredictable signals is also due to the uniqueness of the unpredictable model, and to the large variety of predictable models as the input and learning conditions change.

Frequency Response for Unpredictable Inputs

We must speak finally about frequency response for unpredictable inputs. On the basis of analytical and experimental work done in the Neurology Section of the Massachusetts Institute of Technology, very approximate theoretical frequency response characteristics can be obtained. However, no simulation of the total model response has yet been done.

Using average values from typical tracking situations we have computed

$$\alpha = 10^{-3} \tag{13 a}$$

and

$$\frac{\theta_o}{T}(s) = \frac{10^4}{s(1 + 0.56s)} \tag{13 b}$$

(See Equation 13 *c* and its explanation.)

The magnitude characteristics of the spindle and load are shown in Fig. 30. The gain of the proprioceptor loop is obtained by standard servo approximations. For example, we have closed the loop with a phase margin of only 30°. This is reasonable since we have already observed the low damping of the oscillations in between corrective movements. In considering the visually open loop, we have omitted the intermittency but added a peak at 1.5 cps, as shown in Fig. 31. The loop has then been closed with typical phase margins of 45° and 70°. The effect of the $(1 + k_2 s/k_1)$ term is included as a prefilter which is operative only from 0.5 to 2.5 cps, since at high frequency the operator has only the error to rely upon if he is to follow at all. This approximate prediction of total gain is in agreement with the experimental graphs of Fig. 27. However, simulation should be carried out, since an exact analysis of our model is too difficult. It would also be interesting to look at the impulse responses with reference to the above approximations.

Step Responses

Smith and Cortes made an extensive study of the step response with various large inertia loads and postulated a "bang-bang" model for the human operator, which was optimal for constant force (see Figs. 32 *a* and 32 *b*). Lemay and Westcott (8) started from step response and presented a model (Fig. 29) which included a representation of the arm dynamics as a pure inertia, and a system of samplers for production of a preprogrammed time-optimal step response for constant interval and adjustable force (see Fig. 32 *c*). The predictor was added in order to improve the model's fit to experimental random signal responses, although it would have been more logically added to the model for the known step inputs. The use of constant force instead of constant interval in the time-optimal model introduces only small errors if the inertia load is large; however, our step responses with velocity and acceleration measured–particularly Fig. 12–show a response similar to time-optimal (Fig. 33) for the predictable case, but different for the unpredictable case. Fig. 33 (center) indicates one possible type of action, but Fig. 33 (right) has to be considered as an equally likely possibility. As we shall discuss, physiological data up to now support either of these two modes of response, while we claim the time optimal "bang-bang" model to be valid only for predictable steps.

Intermittency and Psychology

The psychological refractory period and exceptions to it have been described in the literature (5, 6, 7, 18) as well as its application to continuous stimuli (1, 3). Ward, Bekey, Lemay, and Westcott have proposed sampled data models of the human tracker. However, the hand sampler is not as clean as the eye sampler owing to the greater use of prediction in the hand tracking, the higher inertia, and the proprioceptive loop.

Our experiments suggest that intermittency is present for unpredictable inputs, but both our results and physiological considerations suggest it is irregular and asynchronous. The evidence comes from:

(*a*) The ramp experiments,

(*b*) Deterioration of performance such as is shown in Fig. 14 when the frequency of a repetitive signal exceeds 1.5 cps,

(*c*) The refractory period of about 400 msec in short pulse responses,

(*d*) The intermittent corrections in open loop and variable feedback experiments (usually faster, about 4/sec),

(*e*) The peaks in some frequency responses (Fig. 27) at about 1.5 cps, interpretable as half a sampling frequency.

Further observations are:

(*a*) Consistency with unpredictable step responses (Fig. 33).

(*b*) The system is not equivalent to an error-sampled system.

There is always a drive applied to the muscles which consists of pulses from the intermittent process plus signals from the direct input. This explains the diminishing but nonzero ability to track past 1.5 cps.

(*c*) The irregular multiple step responses to a slow ramp are independent of visual tracking. Further, the sampled data control system for the eye (21, 22) has also a velocity servo indicating rather different origins of the control signals to these two complex motor systems.

(*d*) Of interest is the distribution of response times for hand tracking of unpredictable targets: a narrow quasi-gaussian distribution with a mean of 0.24 sec (Fig. 13). This indicates that the sampling times are not clock-driven but rather input-synchronized with some random deviations from the mean. If they were clock-driven one would expect a square distribution (8) between one and two sampling times, perhaps rounded on the corners. This is not found.

Physiological Basis of the Hand Control System

A model of the motor coordination system, particularized to the motion of the supinator and pronator muscles of the forearm, is shown in Fig. 34. The visual loop and the external input are not included.

The pair of muscles, supinator and pronator, is required to rotate the wrist because of the inability of muscles to push; therefore, only one muscle at a time actively aids movement (although the antagonist may be actively braking). The arm load is represented as an inertia, but some force required to overcome the nonlinear apparent viscosity of the muscle is included.

Actuating Elements. The actuating elements are the force generators which control the contraction of the bundles of muscular fibers called motor units. For maximal excitation all motor units (of the order of 10^4) are fired. We call excitation coefficient (α), that fraction of the muscular cross-sectional area that is activated.

Thus, the applied torque becomes αT_{max}. The excitation of the muscle is determined by signals sent from the alpha motor neuron by means of the alpha efferent nerve. These signals originate in the cerebrum, cerebellum, and spinal cord. The alpha motor neuron also receives spindle signals transmitted by the alpha afferent nerve; these signals depend on the length of the pertinent muscle. Other higher center signals come to the spindle through the gamma efferent nerve to control the myotatic or stretch reflex.

The dynamic characteristics of muscles have been studied by Houk and Stark at the Massachusetts Institute of Technology (13). The apparent viscosity has been found to be nonlinear and higher for lengthening than for shortening, thus allowing for quicker damping than by a symmetrical element. The arm muscles can be represented as a linearized block:

$$\frac{\theta_o}{\alpha}(s) = \frac{T_{max}}{s(\beta + Js)} \tag{13 c}$$

where β depends on α.

Spindle. The spindle is a position feedback element connected in mechanical parallel to the muscle. The spindle afferent nerve is connected to a nuclear bag in the center of the spindle. The gamma efferent nerve can contract the spindle fibers, and acts as a level setter. Changes in length or in gamma bias, after being modified by the mechanical dynamics of the tendon, fibers, and nuclear bag, produce contractions in the nuclear bag fibers. These contractions then generate nervous signals which are transmitted to the alpha motor neuron by the spindle afferent nerve. The spindle is highly nonlinear, but the following approximate transfer function has been obtained by Houk for small signals (13):

$$\frac{\alpha_s}{\theta_o}(s) = \frac{k_s\left(1 + \frac{s}{6.8}\right)}{(1 + s/18)(1 + s/200)} \tag{14}$$

The differential behavior over a band of frequencies explains the role of the spindle in the damping of fast movements.

The stretch reflex operates as follows: When a limb is disturbed out of equilibrium, the spindle is stretched and the number of pulses/second sent to the alpha motor neuron is increased. The alpha efferent signal from the alpha motor neuron changes and causes the muscle to move the arm back to equilibrium.

Role of the Proprioceptive Loop. In the model presentation an alternation between voluntary and reflex control of the alpha efferent pathway, the final common pathway, was postulated. The behavior of the motor coordination system would occur as follows: Voluntary movements are preprogrammed in the higher centers and signaled as a whole. At the time of command release (position 1, Figs. 5 *a* and 35 *a*) spindle afferent control is reduced and higher control of the alpha efferents is

fully turned on. The system is operating proprioceptively open loop, characterized by high gain, low damping, and possible postural drift, during a short period of time, about 100 msec. Only apparent viscosity opposes motion; however, regulation comes from proprioceptive feedback and from the apparent viscosity.

After the motion has been substantially completed, the spindle afferent control of the alpha efferent pathway is fully turned on and the gamma efferent may be altered for a new set point; this corresponds to position 2 in Figs. 5 *a* and 35 *a*. The arm may oscillate for a time and is finally clamped to a new position. The new position remains stationary for approximately 230 msec.

If there is still some error, a new correction is applied and the process repeats itself at a rate of some 3 corrections per sec. Fig. 35 *b* presents an alternate model for the action of the alpha motor neuron system which shows the clamping operation to a new value of θ_{ref}. The following figures of merit can be defined:

$$F_{\text{vol}}(s) = \frac{\alpha_o}{\theta_e}(s) = F(s) + \frac{1}{T_{\max} L(s)} \tag{15}$$

$$F_{\text{dist}}(s) = \frac{T_{\text{dist}}}{\theta_e}(s) = F(s) T_{\max} + \frac{1}{L(s)} \tag{16}$$

High $F(s)$ means low direct gain and little stability. Low $L(s)$ means low gain.

This explanation is supported by considerable evidence. For example, the standard finger pointing and finger–nose–finger tests used by neurologists show the open loop nature of rapid movements. Furthermore, lack of antagonist tone during rapid voluntary "freewheeling" movements favors proprioceptive open loop type of control and suggests that the stretch reflex is inoperative during the rapid portion of these movements.

Oscillations up to a few counts per second are possible, and the frequency of oscillation is lower if the subject has to correct for disturbances and the proprioceptive loop is closed (13, 14).

In Parkinson's disease the spindle afferent path cannot be easily switched off, and the corticospinal input is thus weakened. Results are rigidity, inability to track, and low freewheeling frequency (13).

In experiments performed by Stark and Rushworth (13), the gamma input was blocked with procaine. It was found that the initial part of skillful movements (alpha controlled) was still correct, but the termination was severely affected; the subject lost control of his final arm position or of the termination of paper tracing because the proprioceptive feedback path was inoperative for clamping and damping,

Considerations of transient responses, particularly steps (Figs. 12 and 33) also support this dual mode behavior.

CONCLUSIONS

The major conclusions made from our studies are summarized in the model presented (Fig. 5 *a*) for unpredictable inputs.

The evidence for and nature of the intermittency were discussed (Intermittency and Psychology). The dual control of hand movement requires a continual switching process from postural to voluntary systems. This determines which of the two modes has control of the final common path, the alpha motor neuron. This phenomenon provides the intermittency, which was shown to be input synchronized.

The action of the hand system as a position servo and the absence of a velocity servo were also shown, by ramp and also by open loop experiments; in contrast to the eye movement tracking, the hand system can usually, although not always, adapt itself to the last, bizarre change in experimental arrangement.

The distinction between predictable and unpredictable inputs was shown with regard to some pitfalls in human engineering literature, to the frequency response, and to the transient responses.

Received for publication 15 December 1966 and in revised form 28 August 1967.

FIGURES

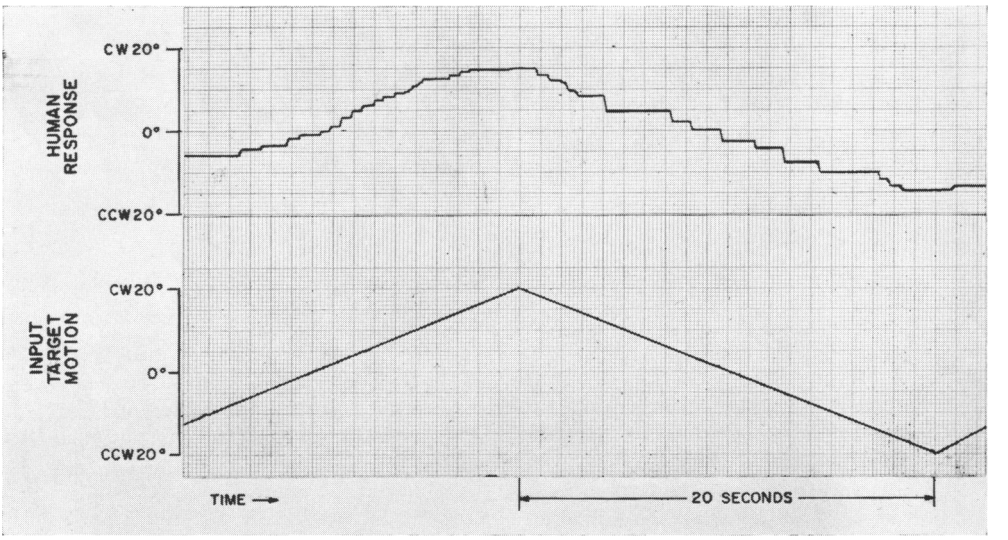

FIGURE 1 Discontinuous change of hand position to slow target ramps. CW, clockwise; CCW, counterclockwise.

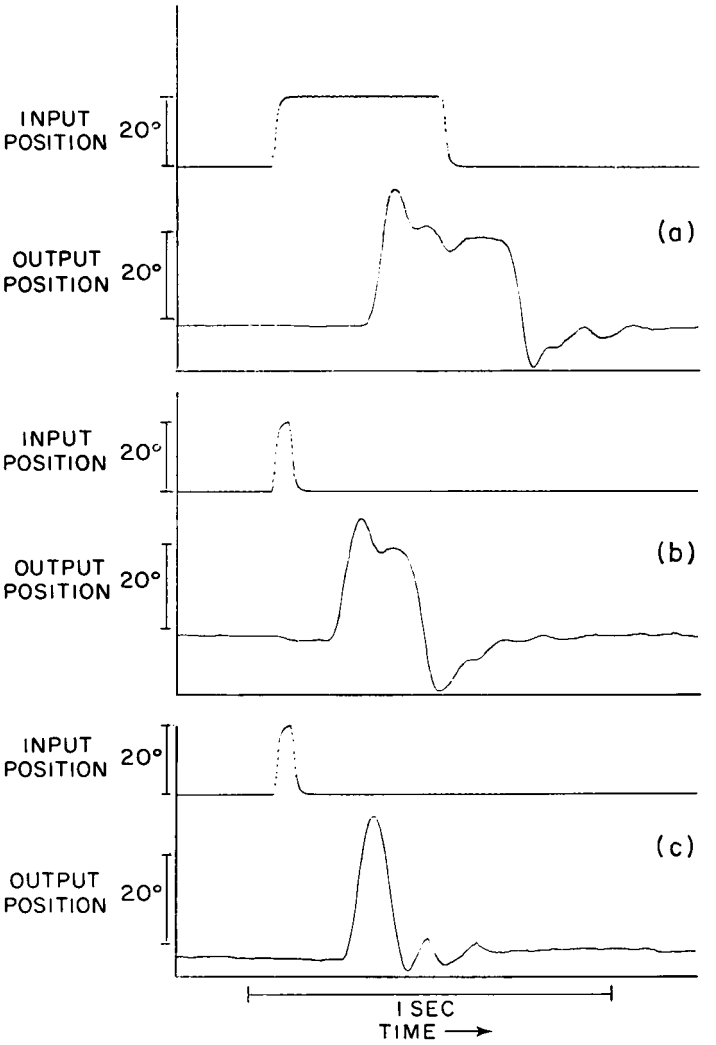

FIGURE 2 Responses to unpredictable wide pulse, unpredictable narrow pulse, and predictable narrow pulse showing respectively, delay, refractory period, and input-adapted preprogramming.

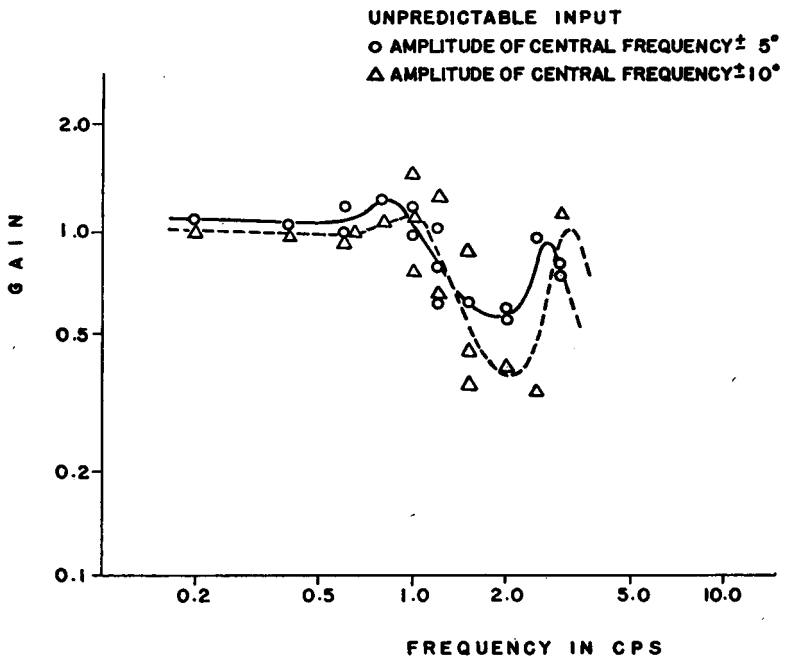

FIGURE 3 Effect of amplitude on frequency response gain data.

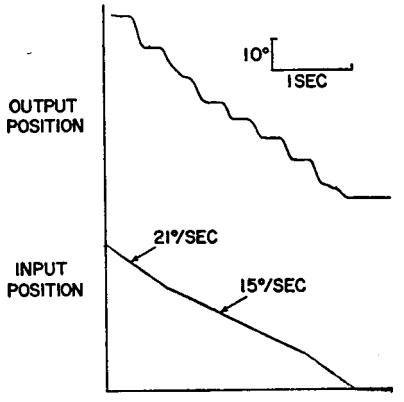

FIGURE 4 Intermittent response to unpredictable ramp inputs.

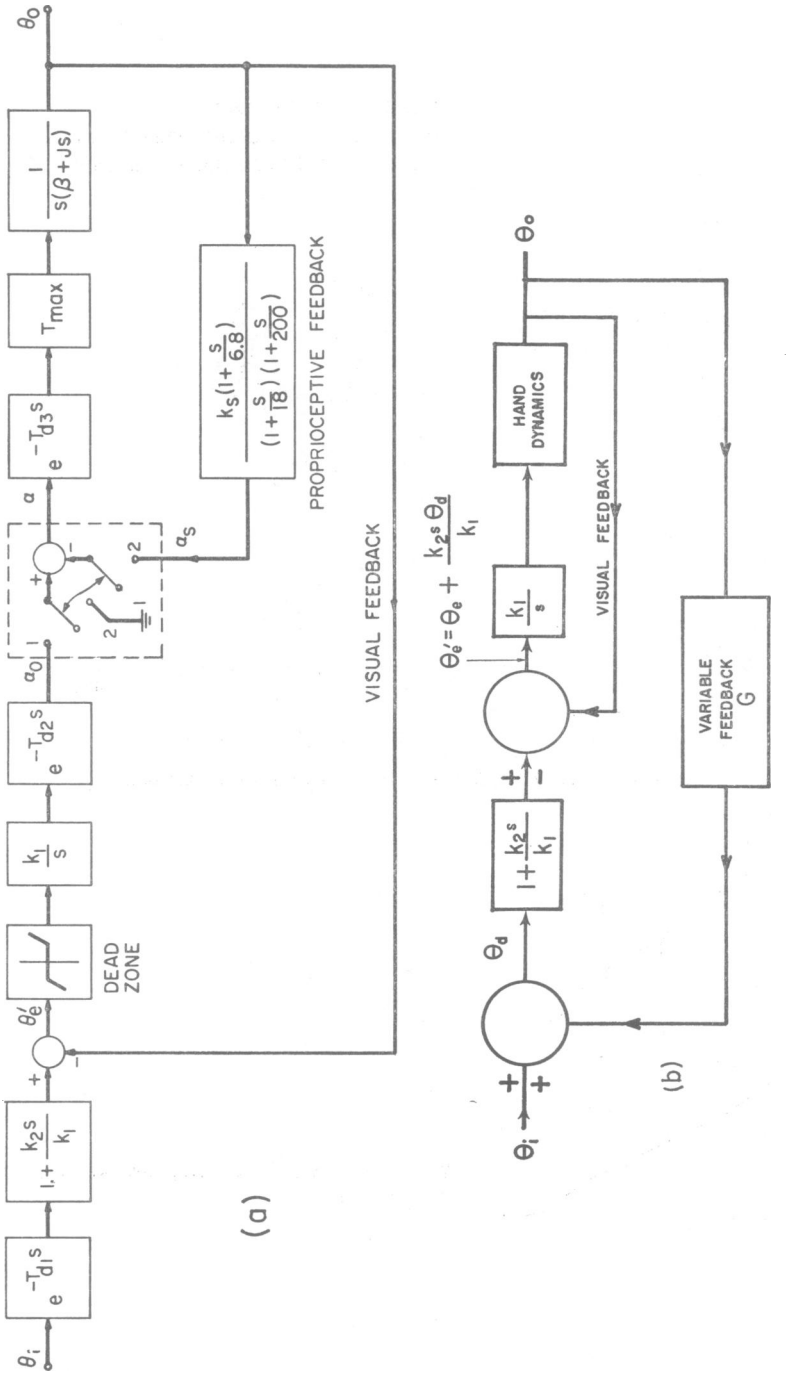

FIGURE 5 (*a*) Model for pursuit tracking of unpredictable inputs. (*b*) Open loop and variable feedback arrangement.

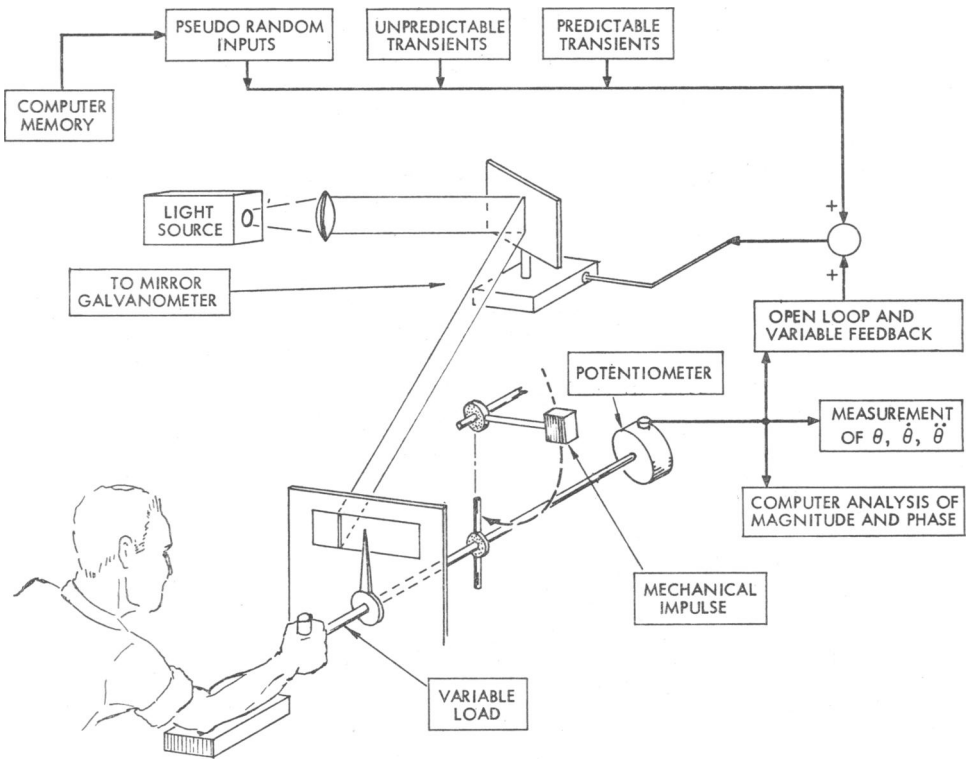

FIGURE 6 Sketch of apparatus.

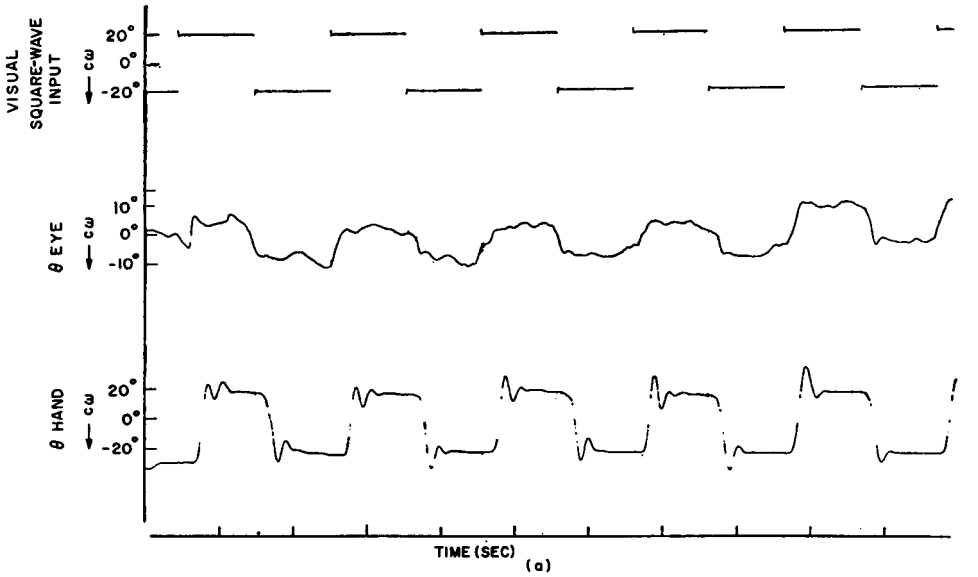
VISUAL SQUARE-WAVE INPUT
20°
0°
-20°
cω
θ EYE
10°
0°
-10°
θ HAND
TIME (SEC)
(a)

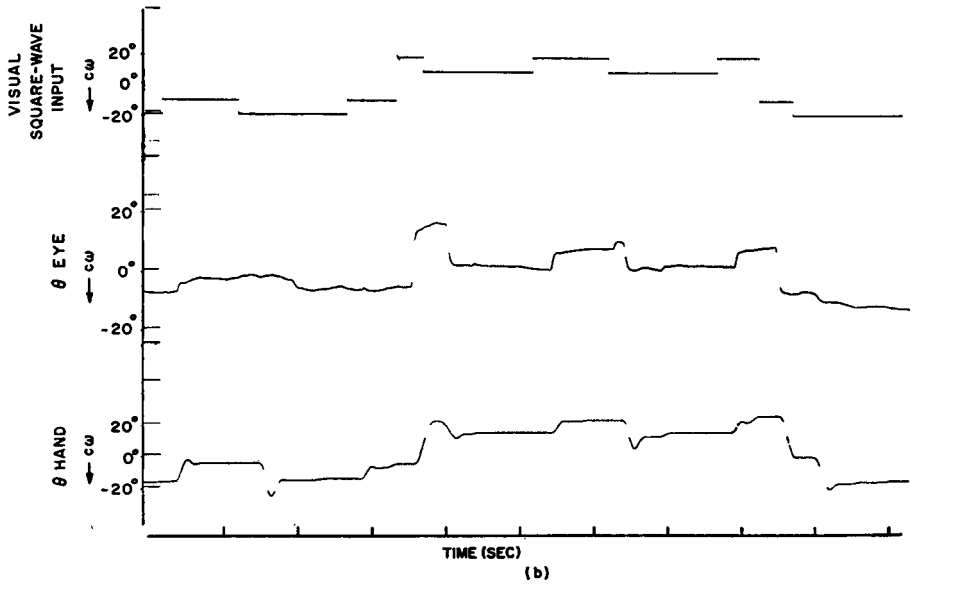
VISUAL SQUARE-WAVE INPUT
20°
0°
-20°
θ EYE
θ HAND
TIME (SEC)
(b)

FIGURE 7 *a, b*

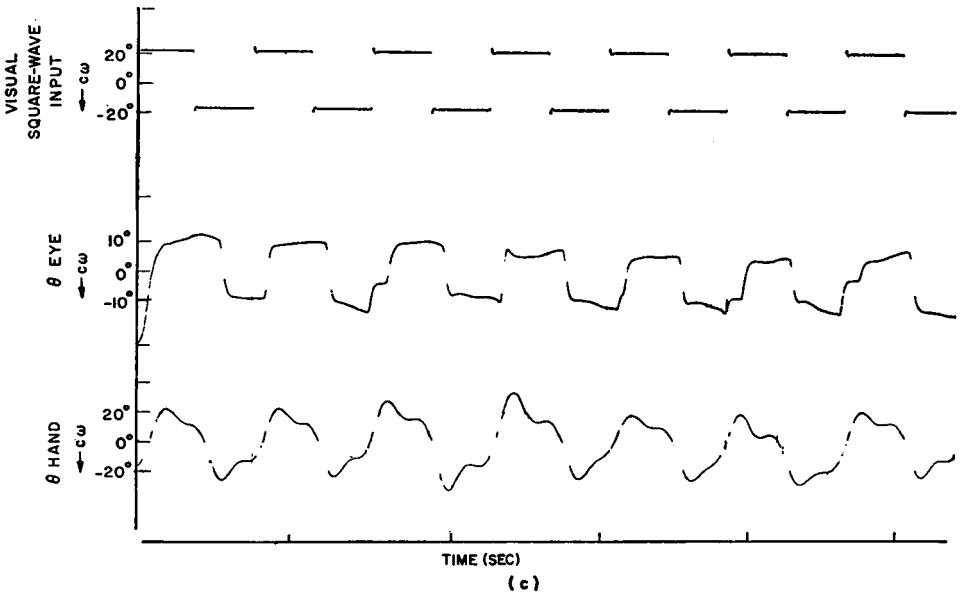

FIGURE 7 *a, b, c* Eye and hand step responses to random (*b*) and regular target square waves (*a*) 0.5 cps and (*c*) 2.5 cps.

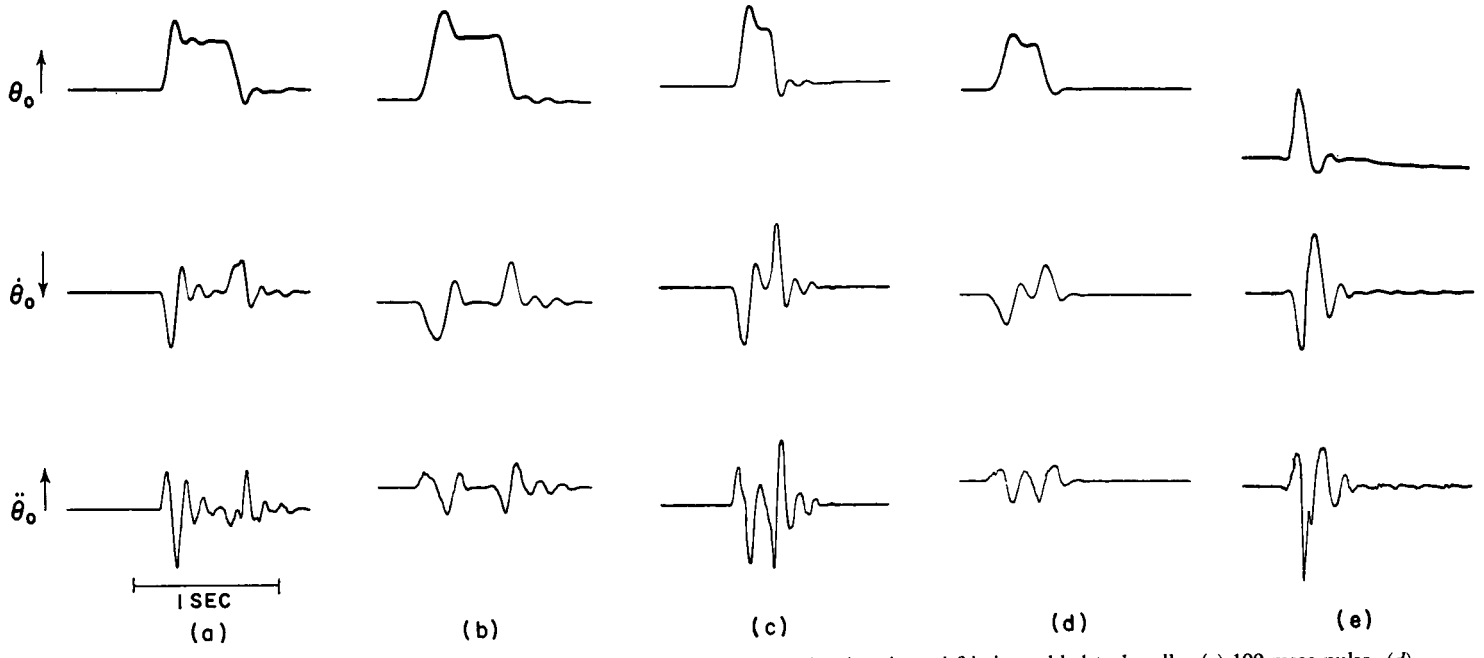

FIGURE 8 Responses to pulse inputs: (*a*) 400 msec pulse; (*b*) 400 msec pulse, inertia and friction added to handle; (*c*) 100 msec pulse; (*d*) 100 msec pulse, inertia and friction added to handle; and (*e*) predictable input, response to 100 msec known pulse.

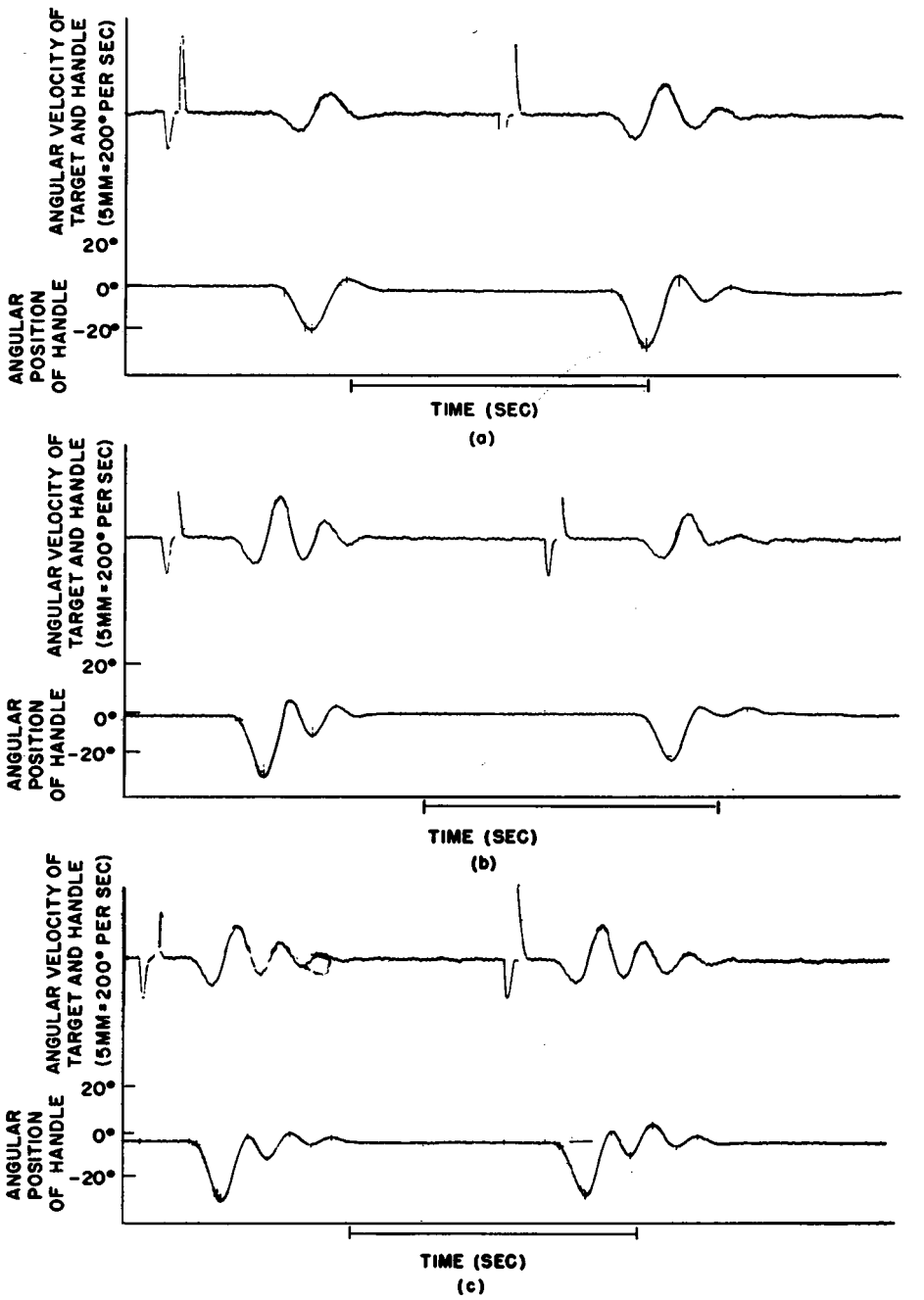

FIGURE 9 Visual impulse responses with velocity indicated: (*a*) relaxed condition; (*b*) moderately tense condition; and (*c*) very tense condition.

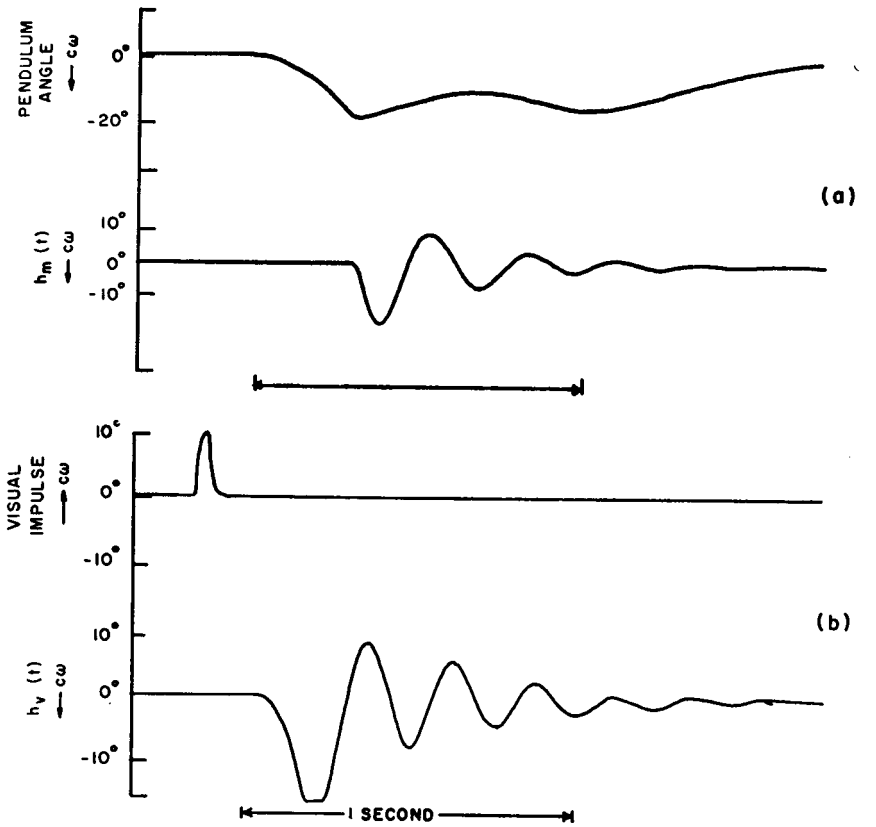

FIGURE 10 Impulse experiments. Top trace: input signals; bottom trace: mechanical impulse responses $h_m(t)$, or visual impulse response, $h_v(t)$. (*a* and *b*) relaxed; (*c* and *d*) tense condition.

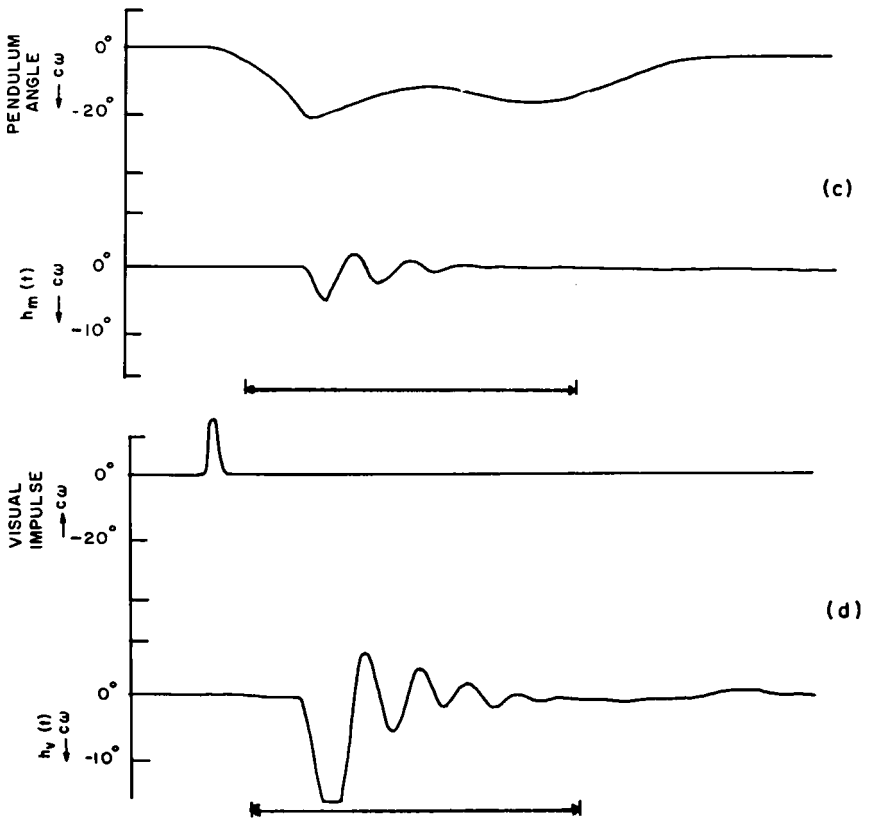

FIGURE 10 *c, d*

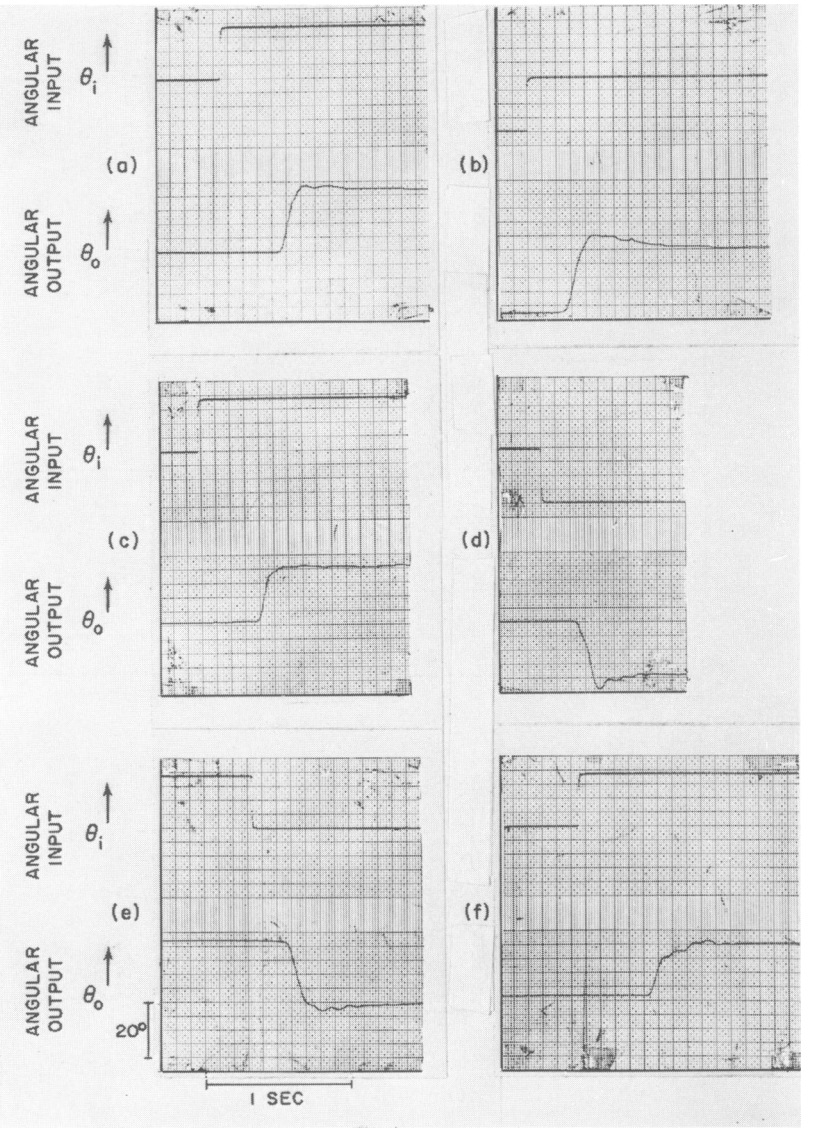

FIGURE 11 Six types of step response: (*a*) 11 cases out of 40; (*b*) 7 cases; (*c*) 7 cases; (*d*) 5 cases; (*e*) 5 cases; and (*f*) 3 cases.

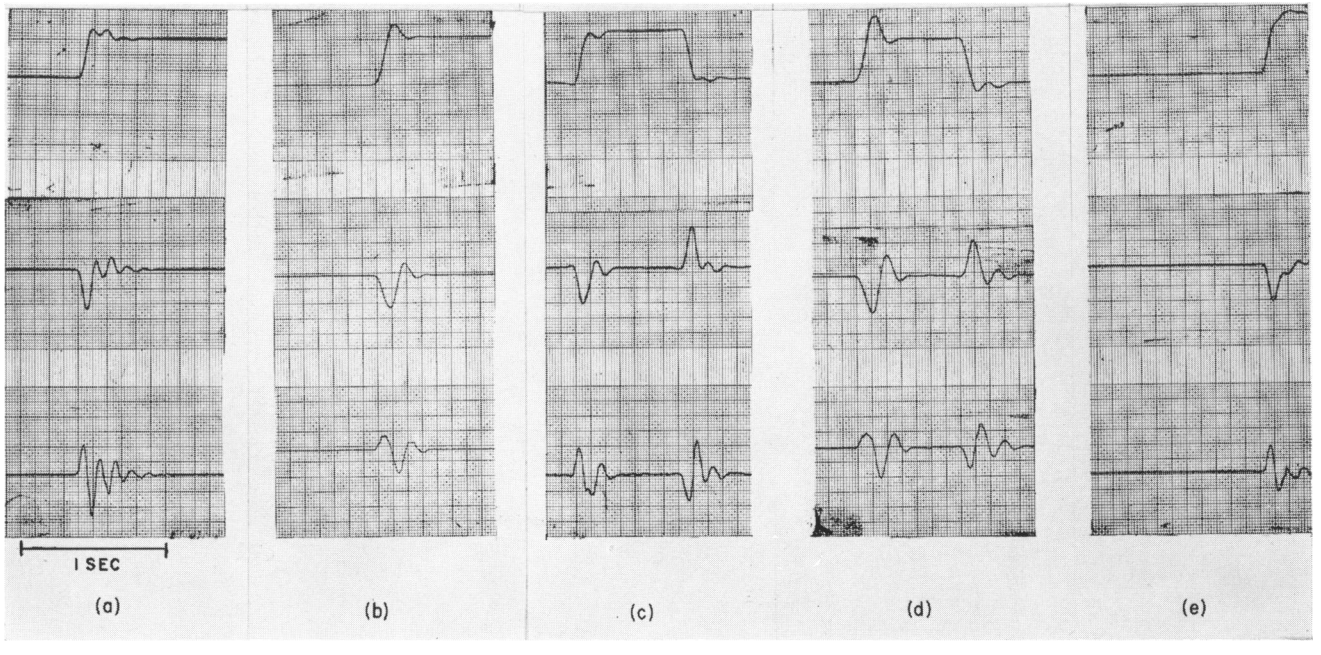

FIGURE 12 Step responses: (*a*) and (*b*) unpredictable; (*c*) and (*d*) unpredictable with inertia and friction added to handle; and (*e*) predictable–response to known step after training. Upper trace is position. Middle trace is inverted velocity. Lower trace is acceleration.

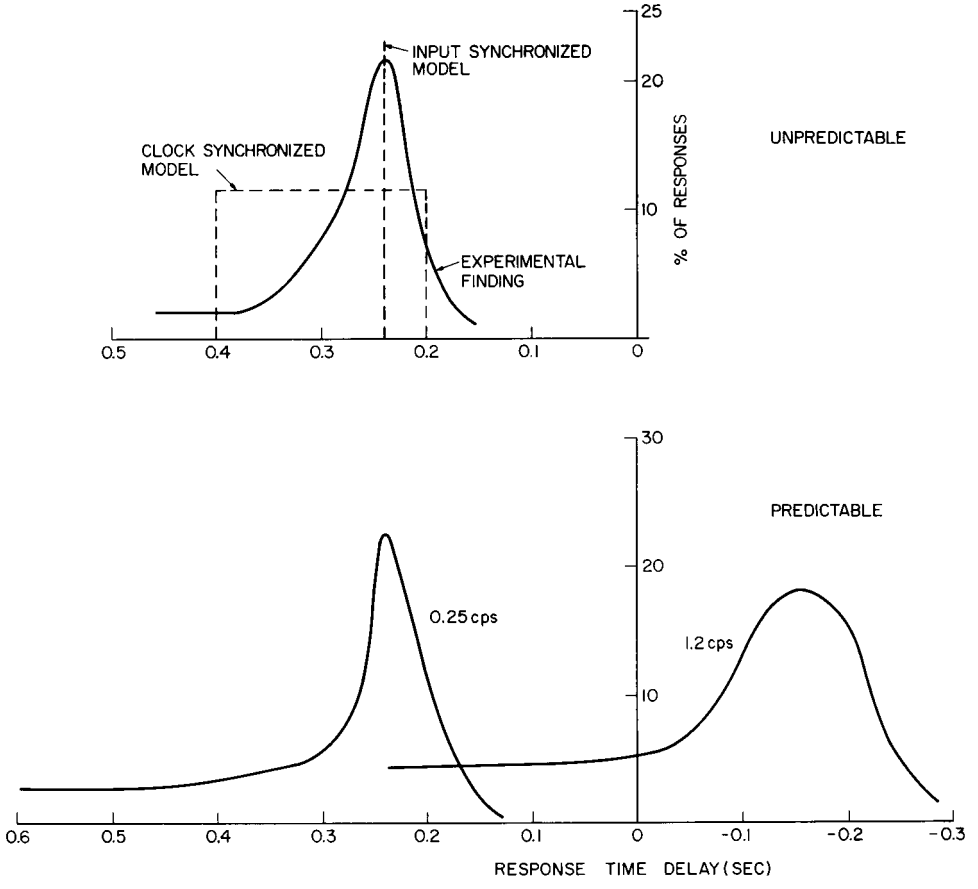

FIGURE 13 Reaction time distributions for responses to both unpredictable steps and predictable square waves.

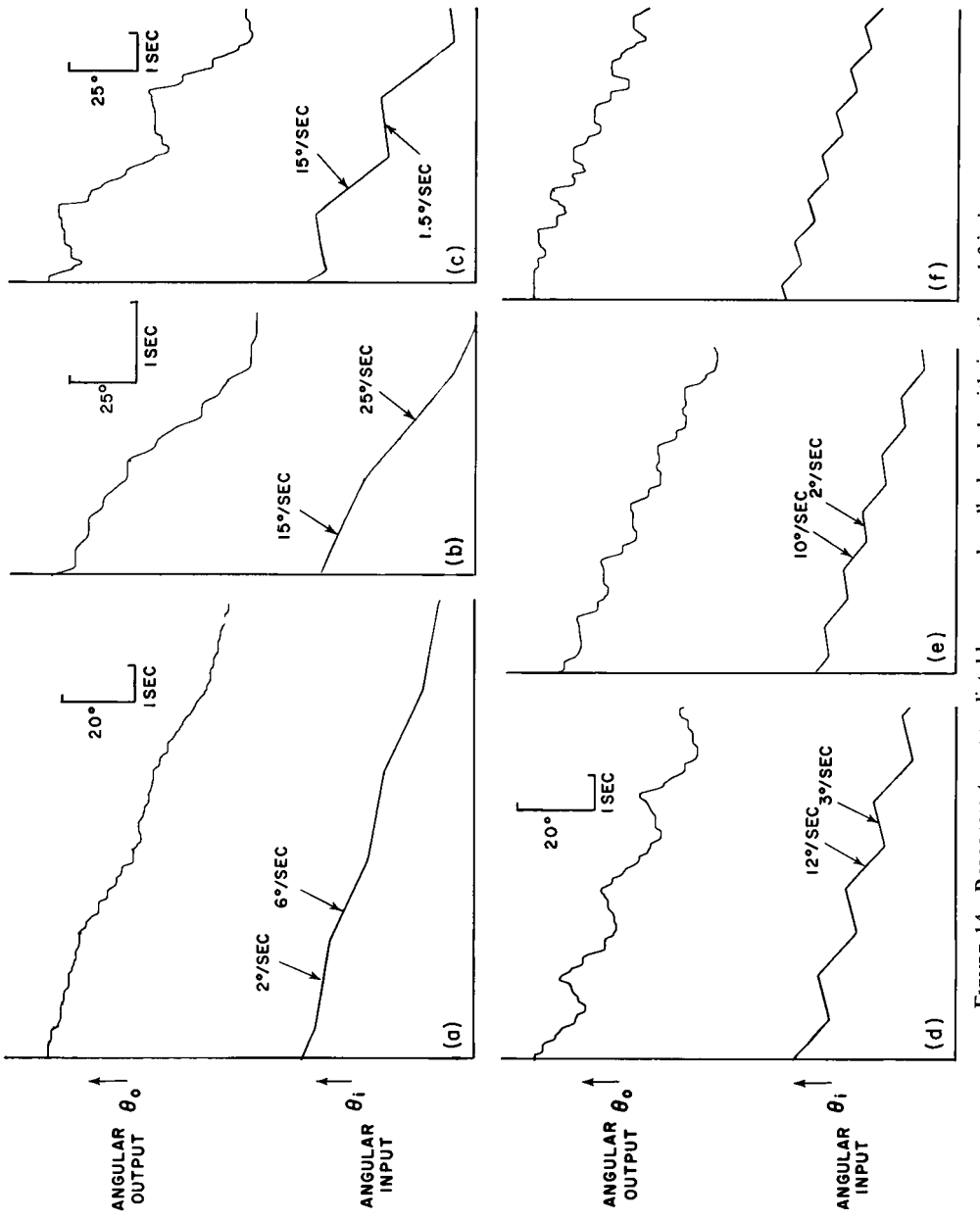

FIGURE 14 Responses to unpredictable ramps, handle loaded with inertia and friction.

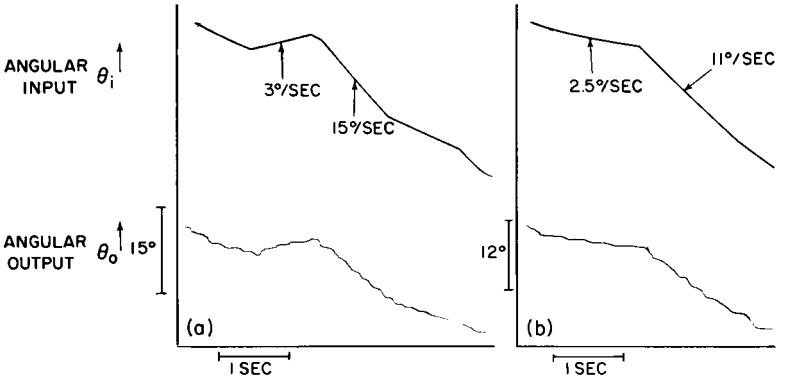

FIGURE 15 Responses to unpredictable ramps.

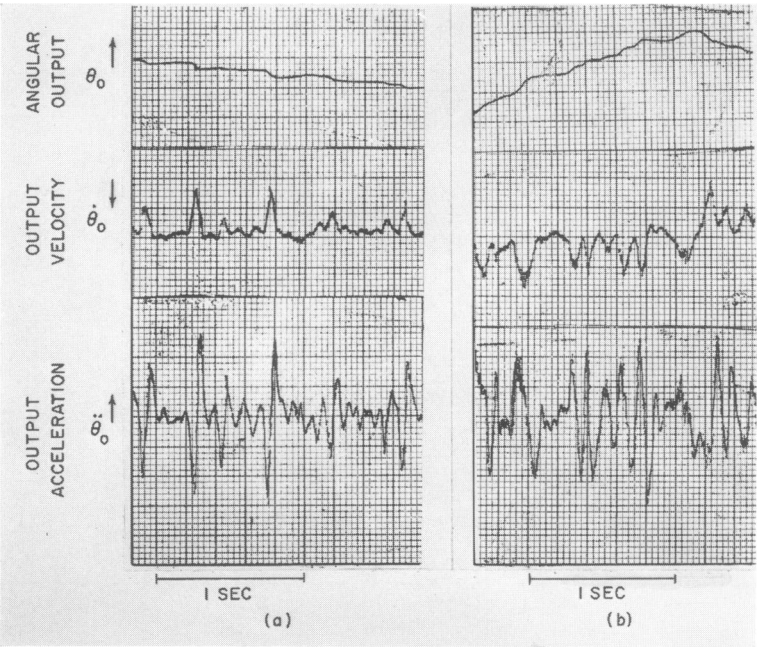

FIGURE 16 Ramp responses with output velocity and acceleration indicated.

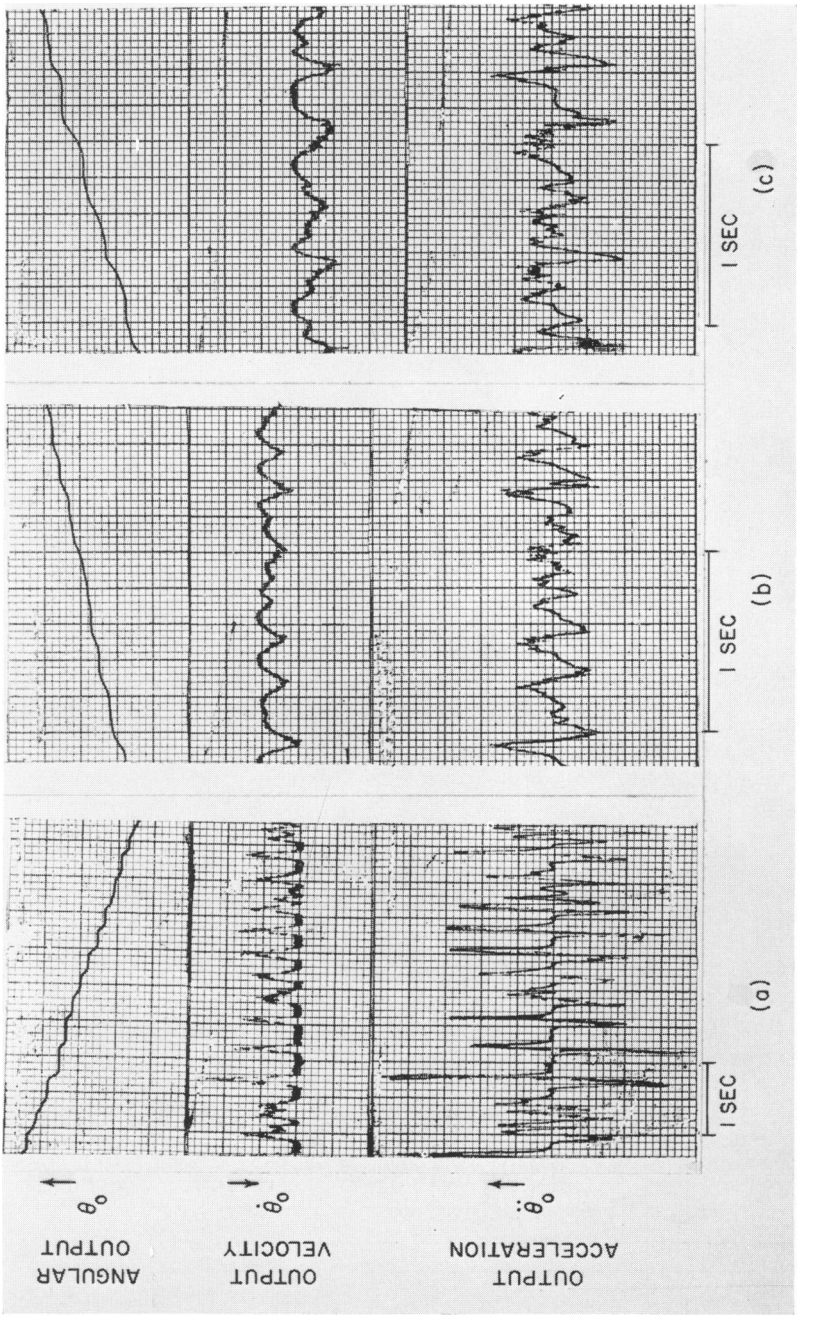

FIGURE 17 Ramp responses with output velocity and acceleration indicated, handle loaded with inertia and friction.

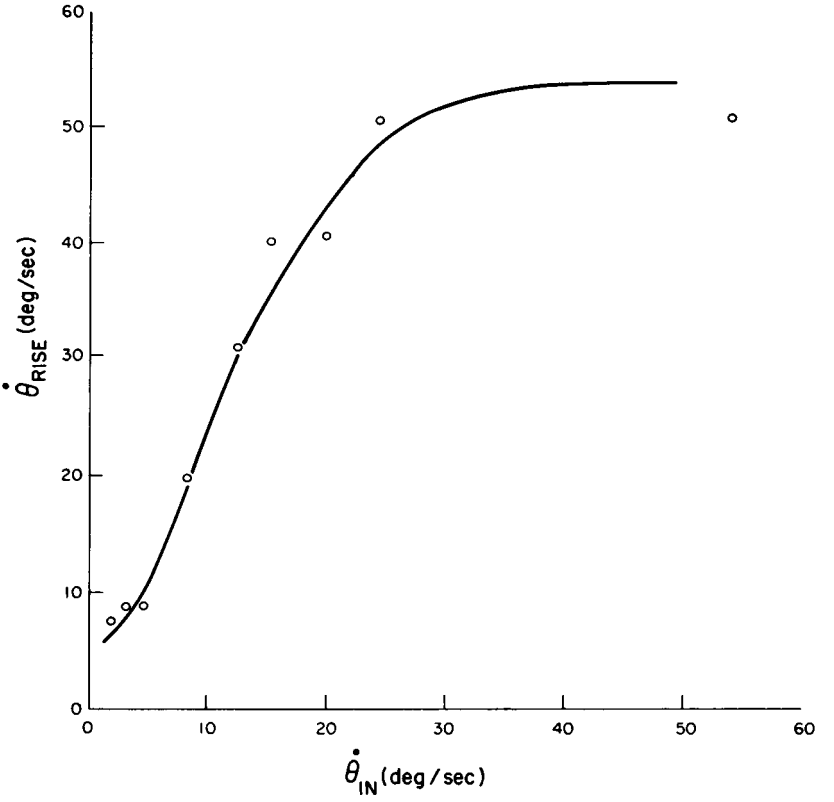

FIGURE 18 Quasi-linear relationship between saccadic rise velocity and input velocity (random ramp input).

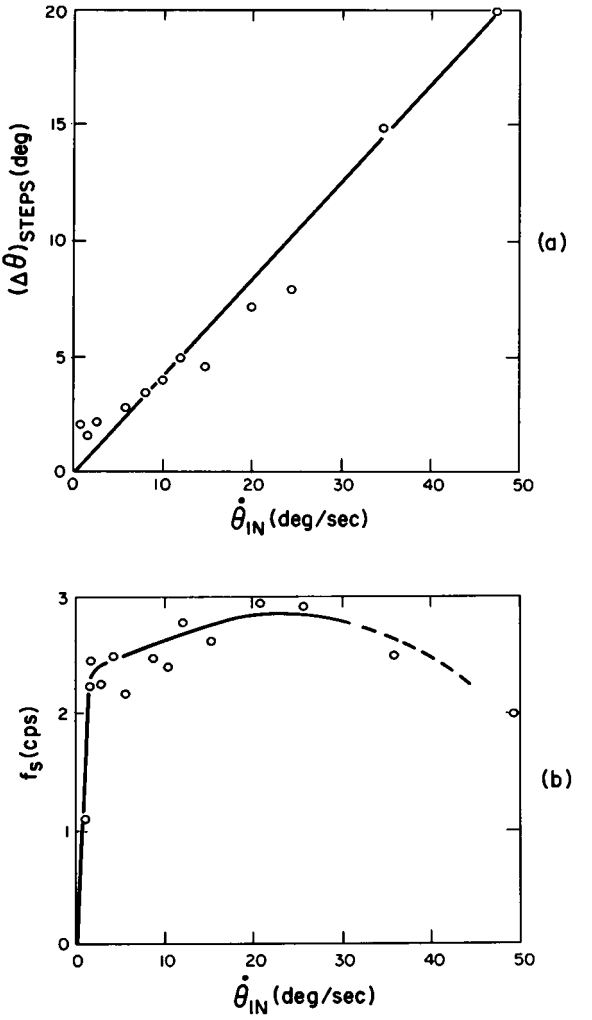

FIGURE 19 (*a*) Size of intermittent response as a function of input velocity. (*b*) Frequency of intermittency as a function of input velocity.

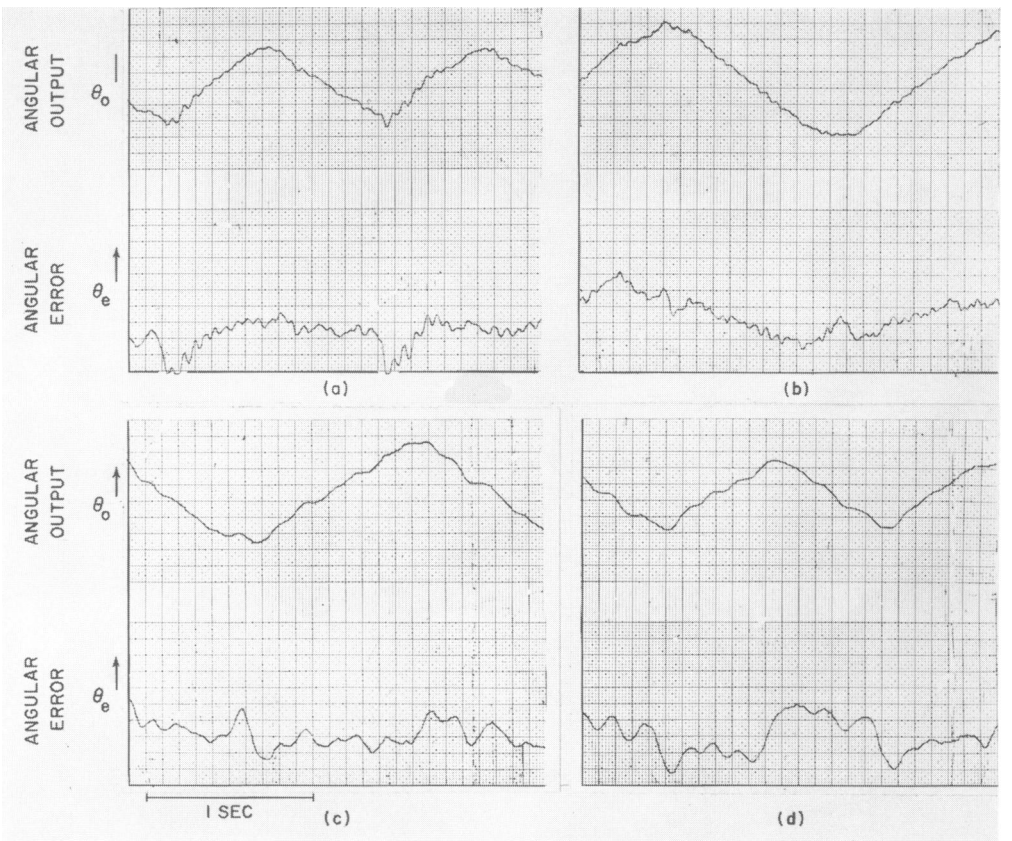

FIGURE 20 Output and error for ramp inputs, tense conditions (*a*) and (*b*); relaxed conditions (*c*) and (*d*).

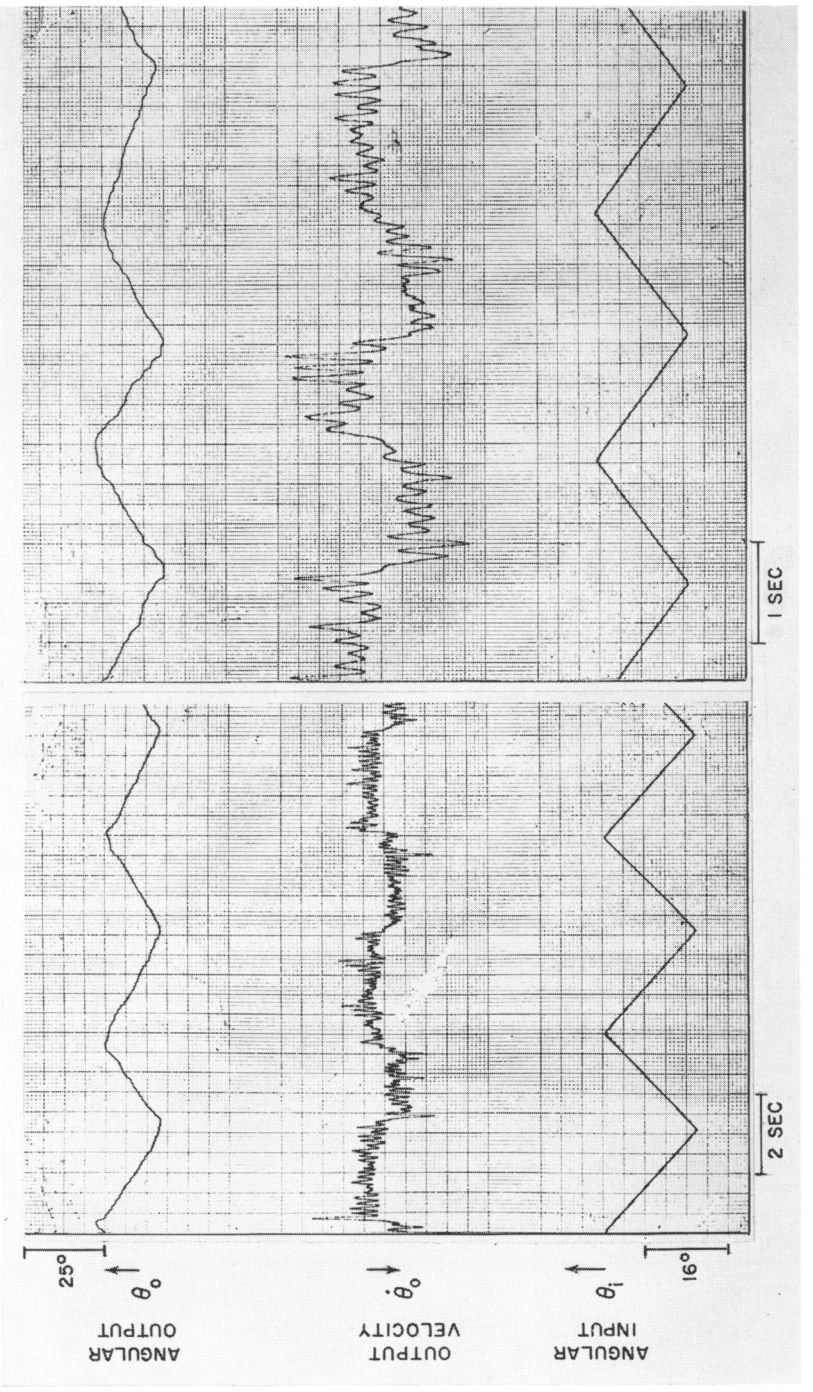

FIGURE 21 Response to known 8°/sec and 14°/sec ramps.

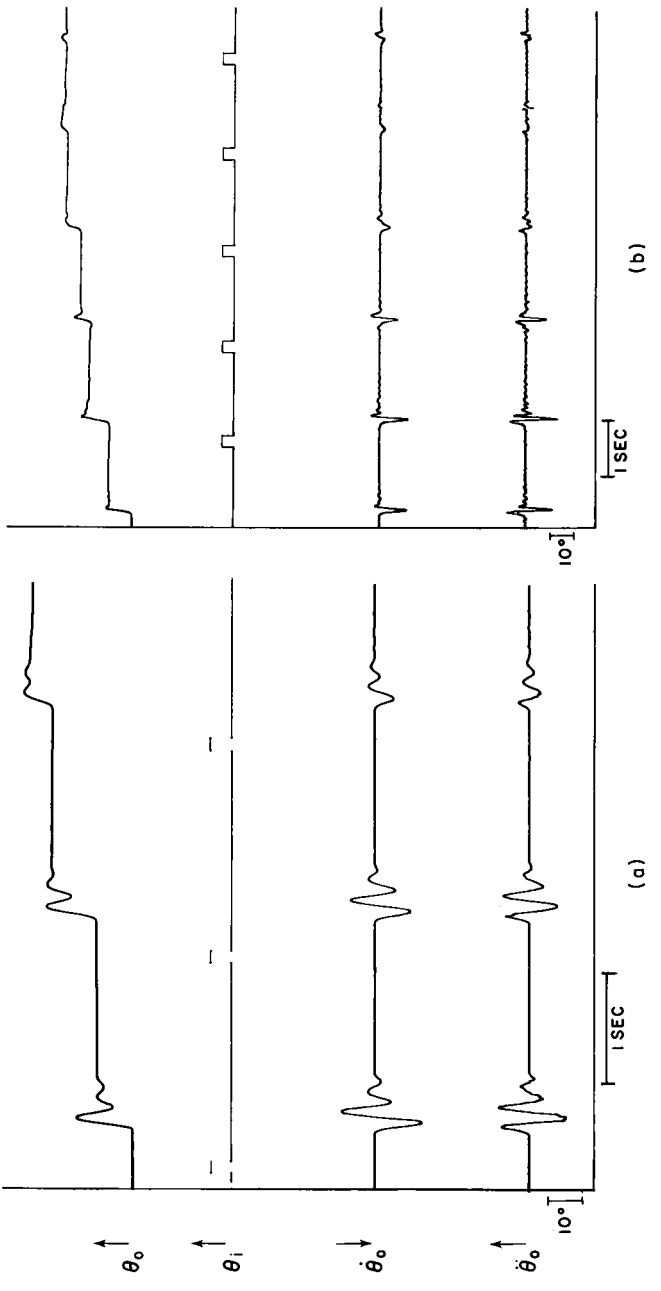

FIGURE 22 Pulse responses of open loop system. Upper trace: output position. Next trace: input. Next trace: inverted output velocity. Lowest trace: output acceleration.

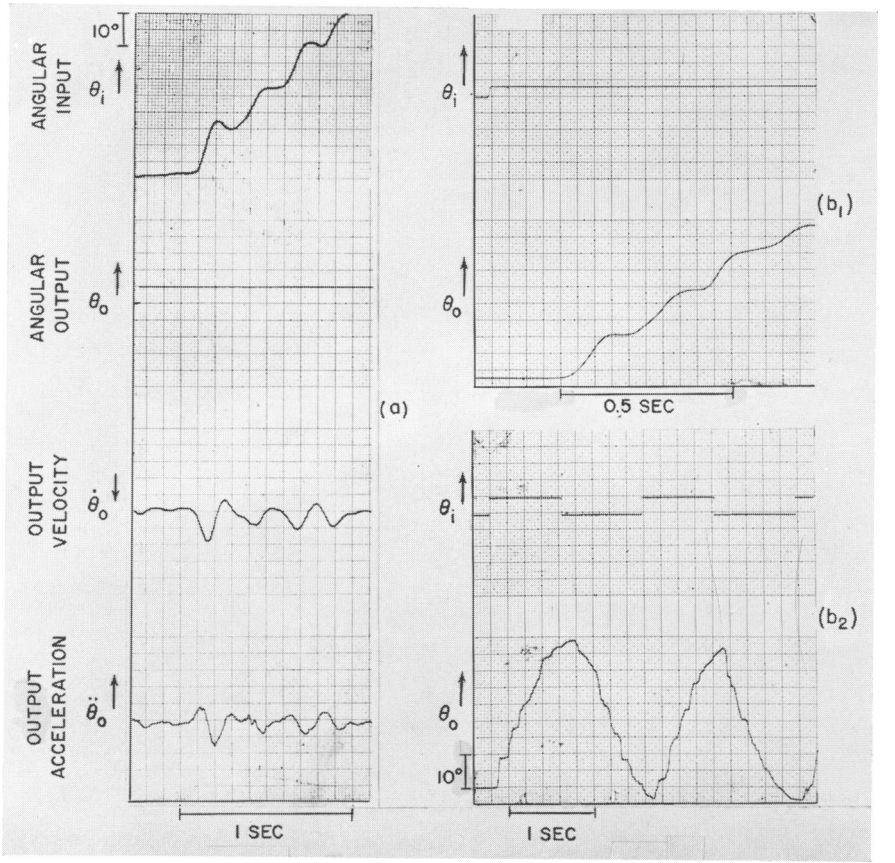

FIGURE 23 Step responses of open loop system, loaded handle. (*a*) output, input, inverted output velocity, and output acceleration; (b_1 and b_2) upper trace input position, lower trace output position.

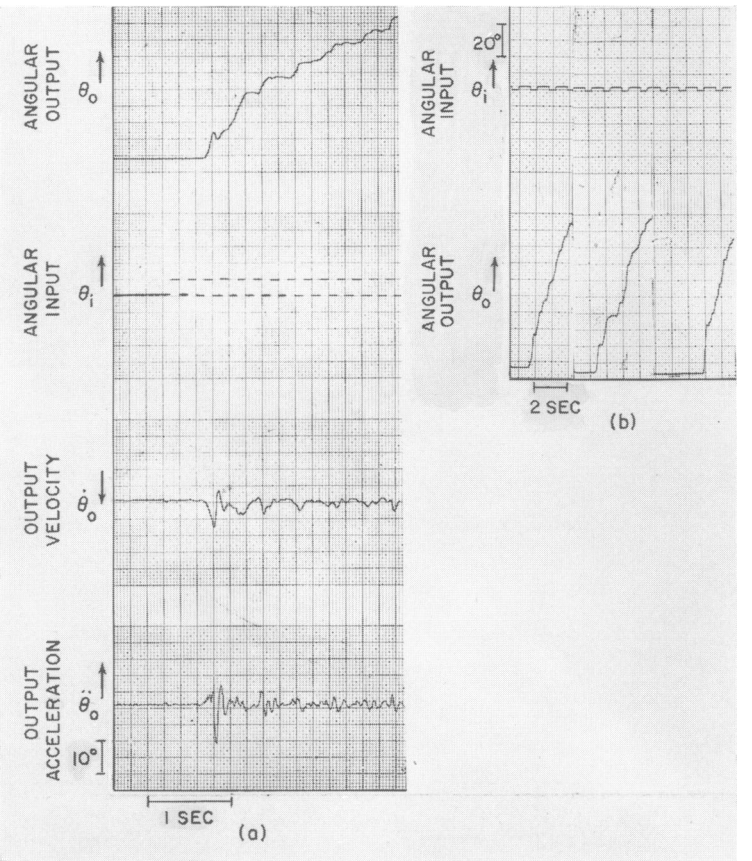

FIGURE 24 Open loop system. Responses to high repetition square waves; analogous to step responses. (*a*) output, input, inverted output velocity, and output acceleration; (*b*) upper trace input position, lower trace output position.

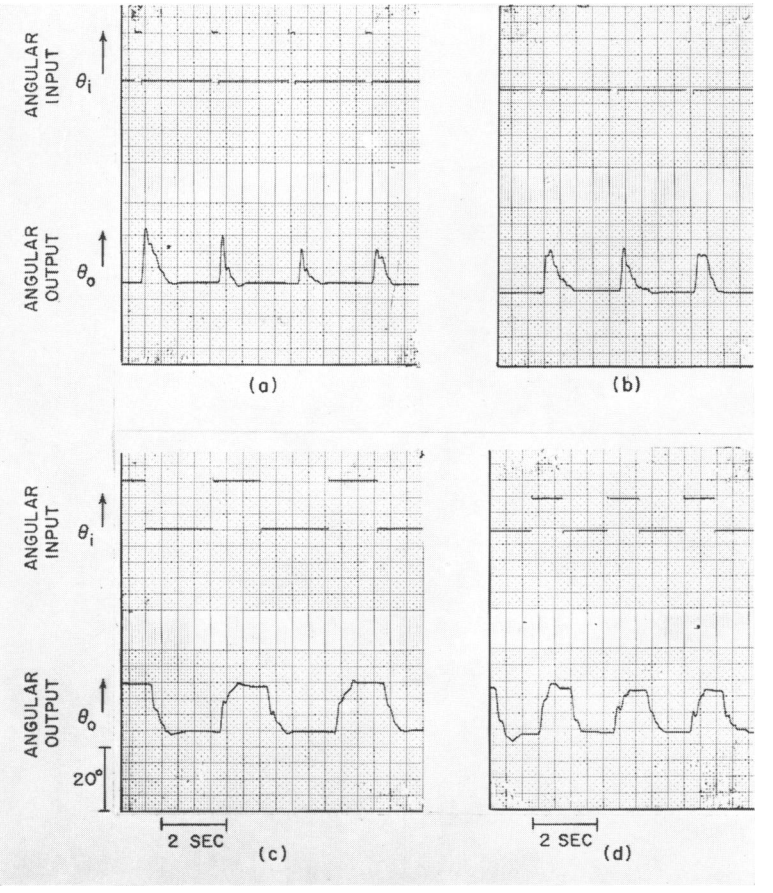

FIGURE 25 (*a*) Pulse response with $G = \frac{1}{2}$; (*b*) Pulse response with $G = \frac{2}{3}$; (*c*) Step response with $G = \frac{1}{2}$; and (*d*) Step response with $G = \frac{2}{3}$. For definition of G see Fig. 5 *b*.

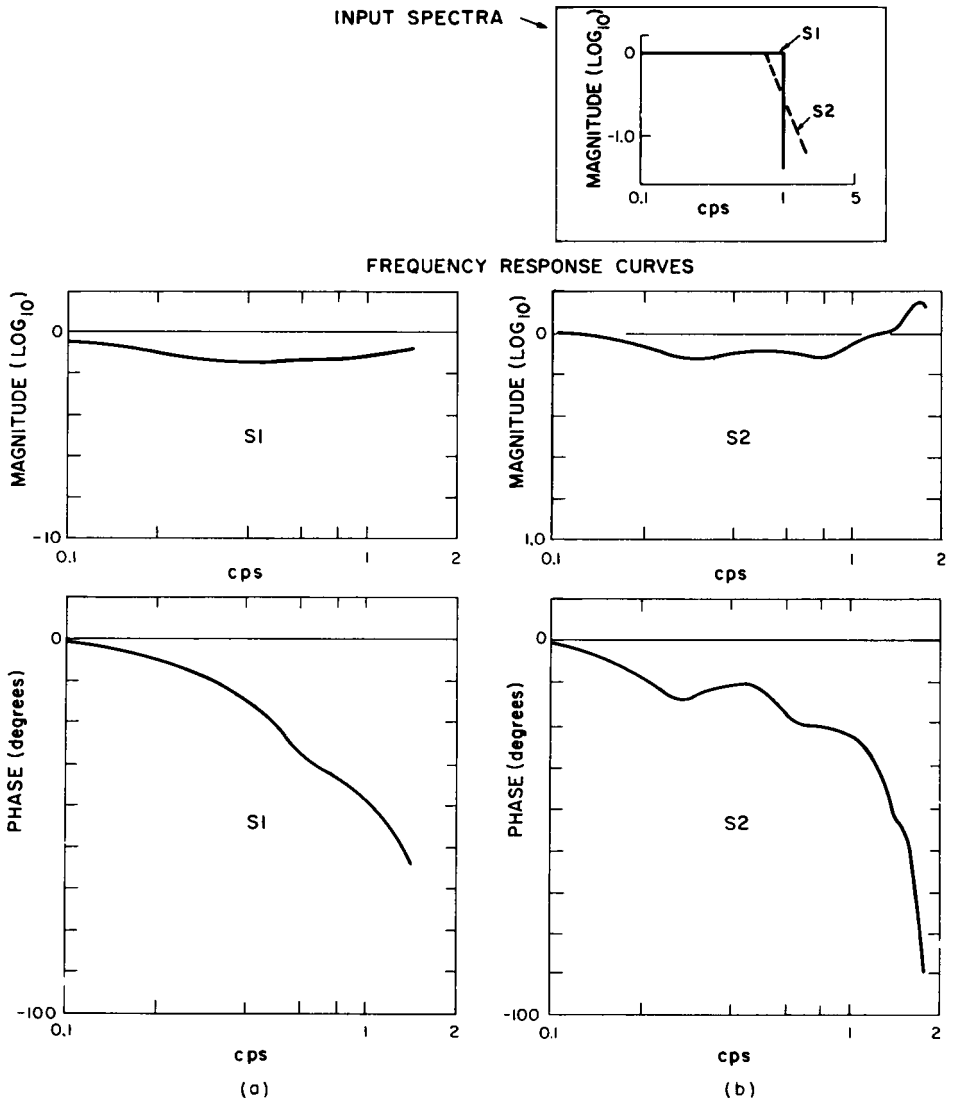

FIGURE 26 Frequency responses to quasi-random continuous signals. Input spectrum shown.

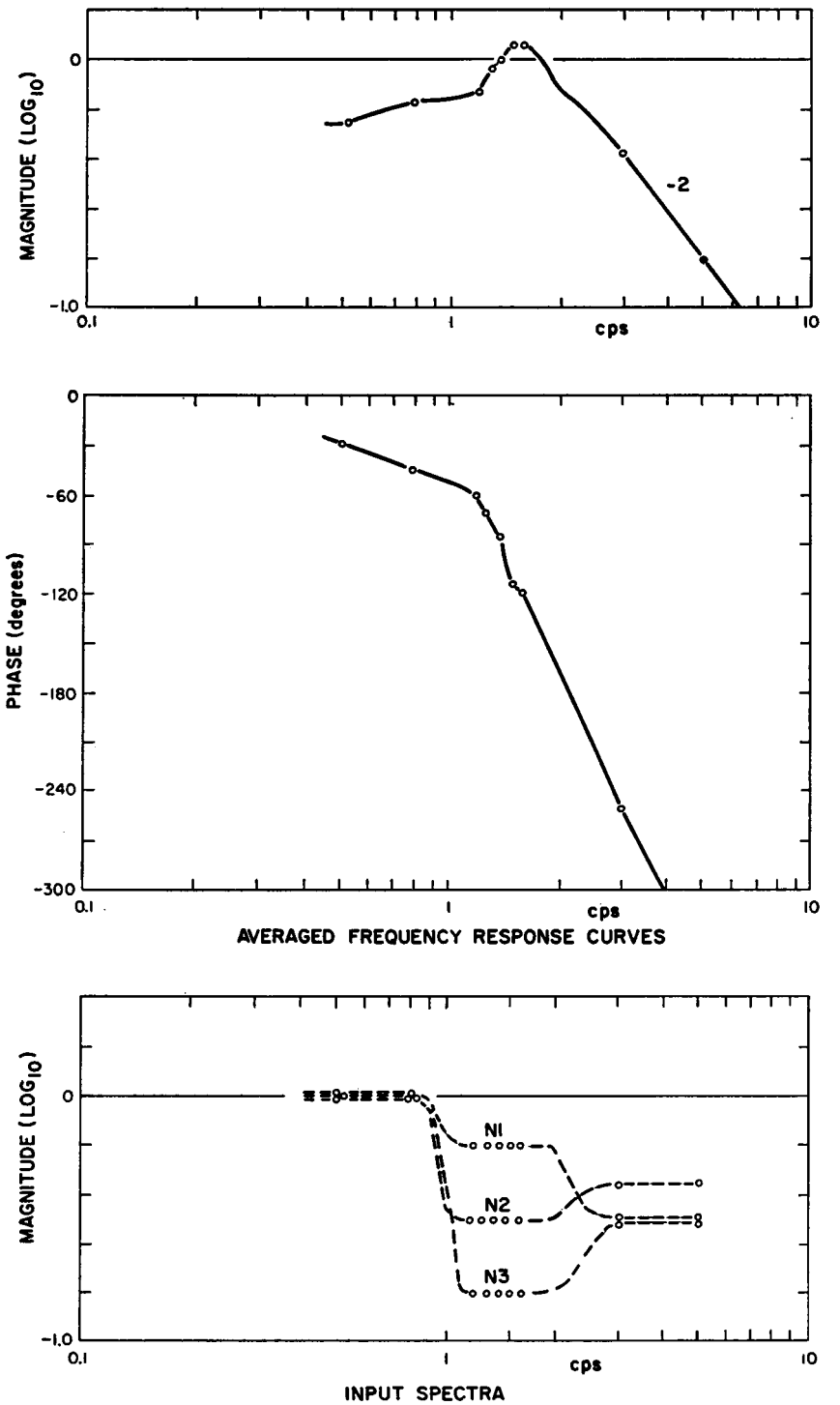

FIGURE 27 Average frequency response to quasi-random continuous signals. Input spectrum shown.

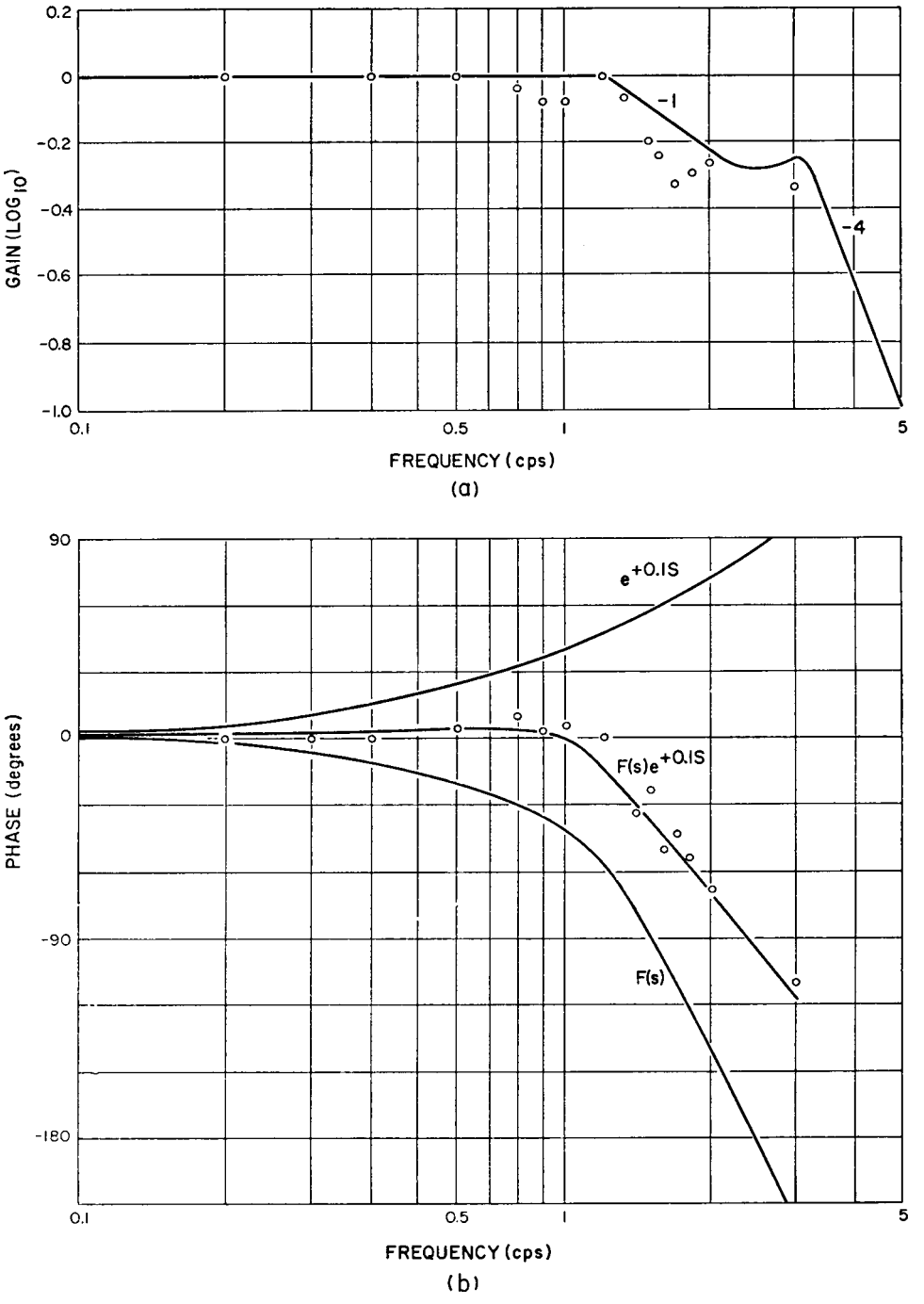

FIGURE 28 Frequency response to closed loop predictable sinusoidal inputs and fit by a transfer function.

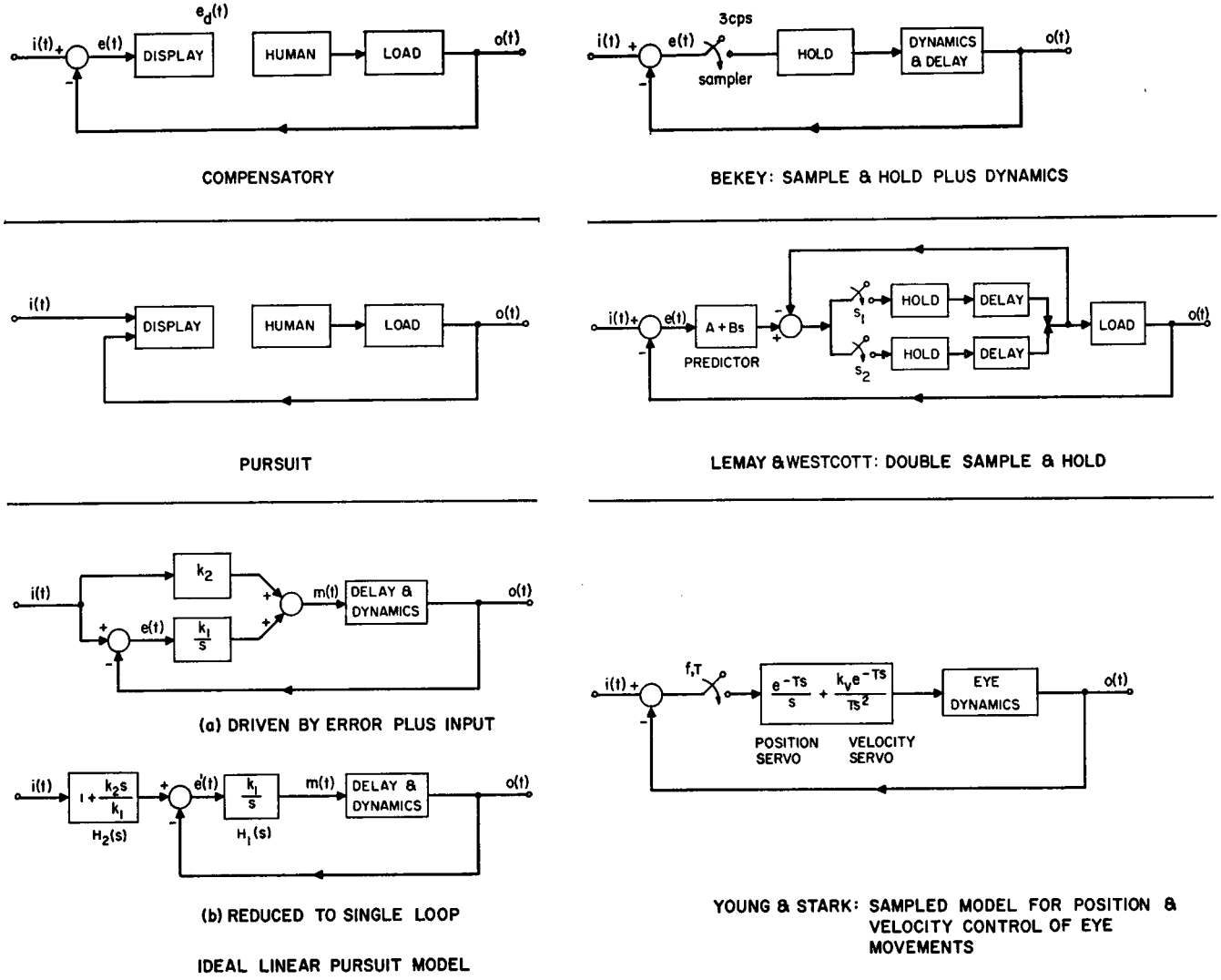

FIGURE 29 Other continuous and discontinuous models for hand tracking.

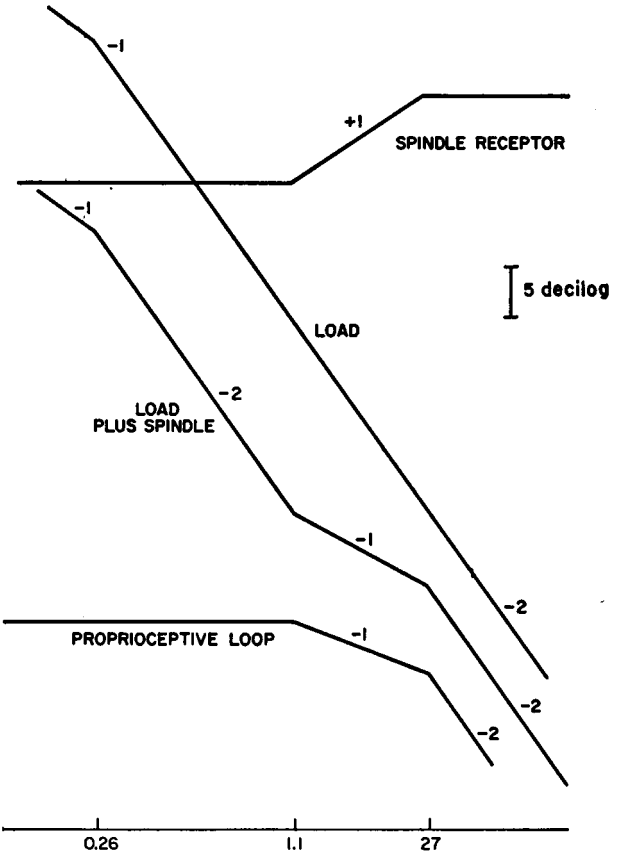

FIGURE 30 Frequency characteristics of proprioceptive loop model.

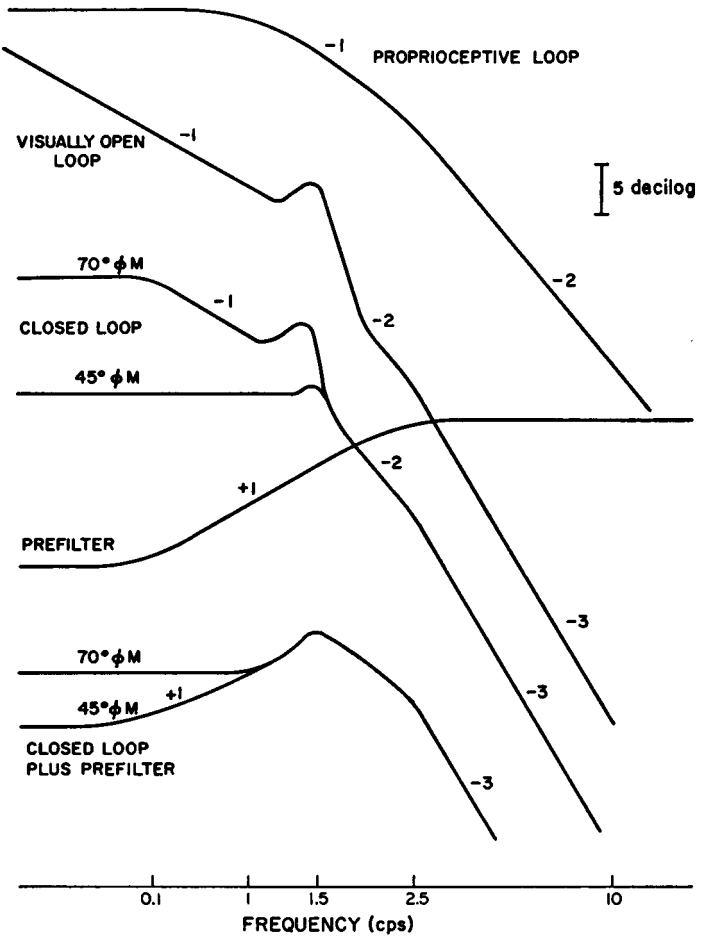

FIGURE 31 Frequency characteristics of the complete unpredictable tracking system model.

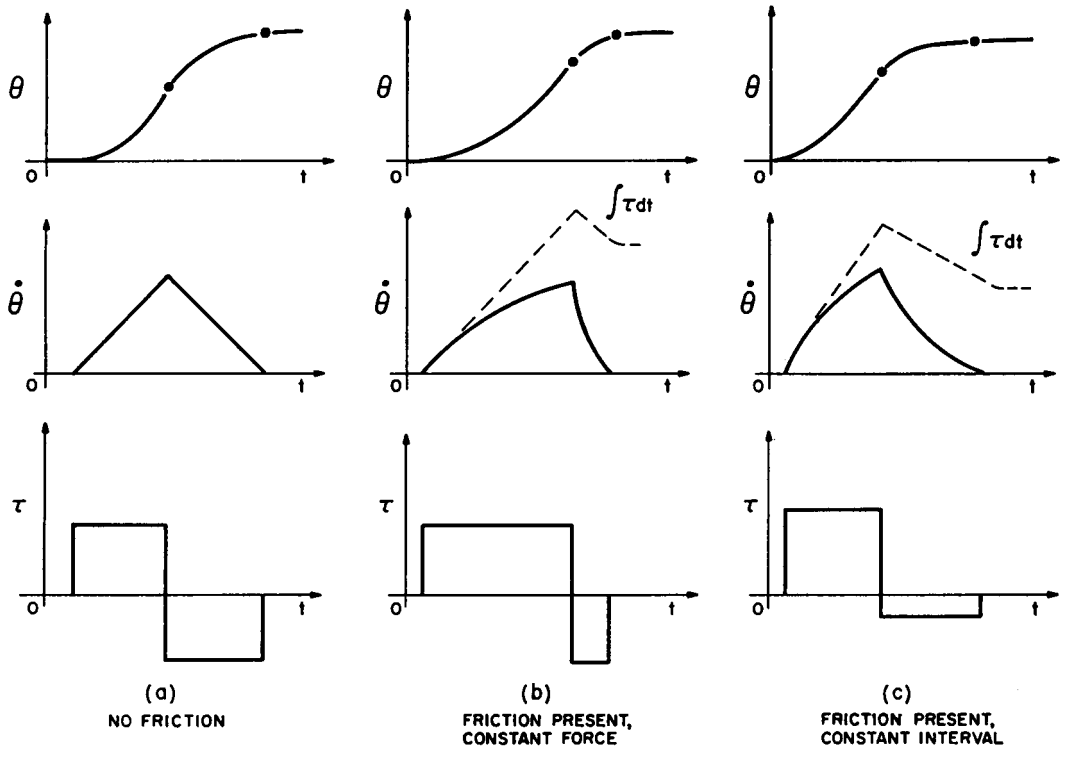

FIGURE 32 Time optimal step responses.

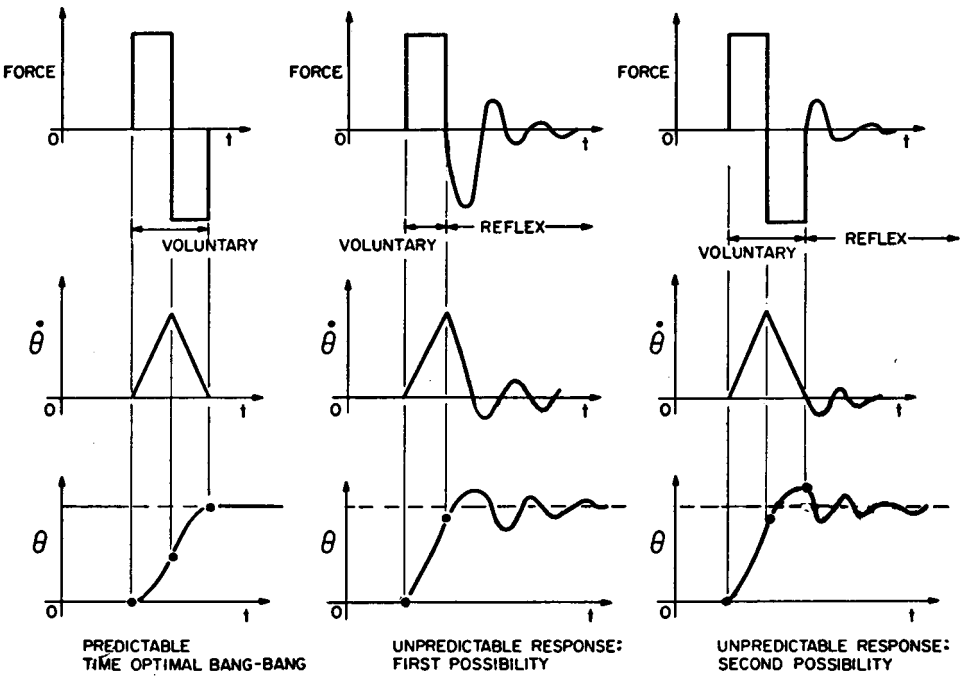

FIGURE 33 Possible types of ballistic movements.

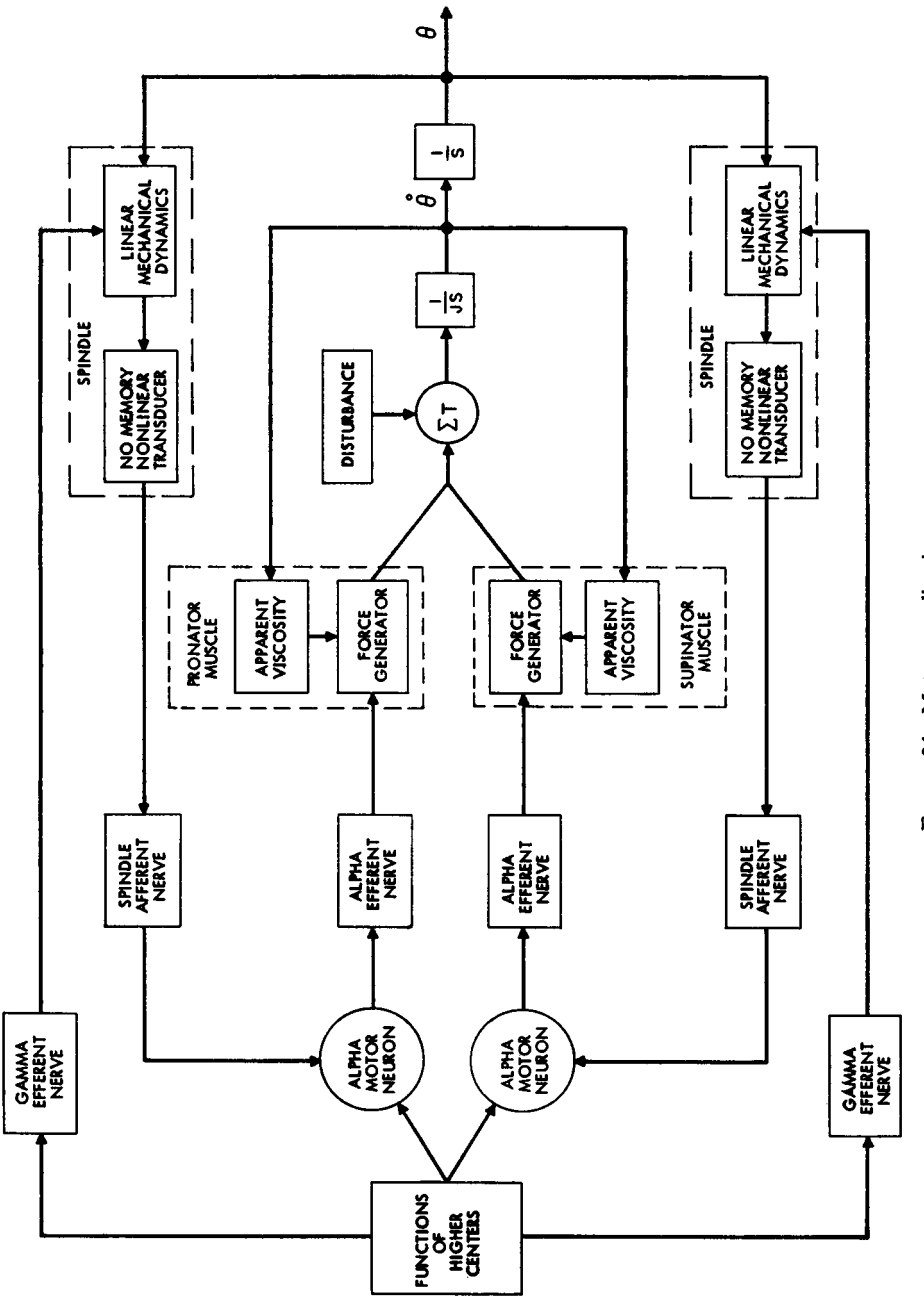

FIGURE 34 Motor coordination system.

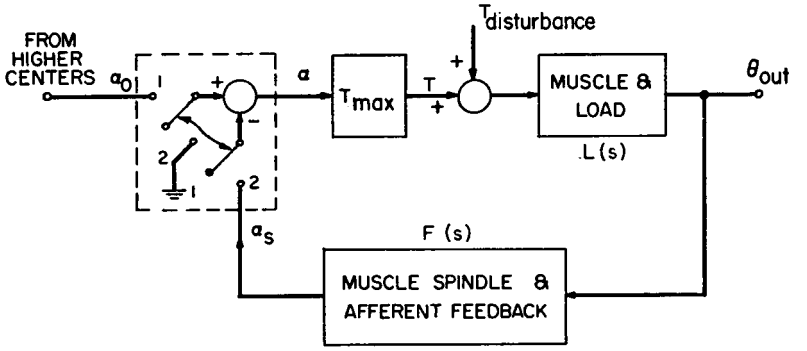

(a)

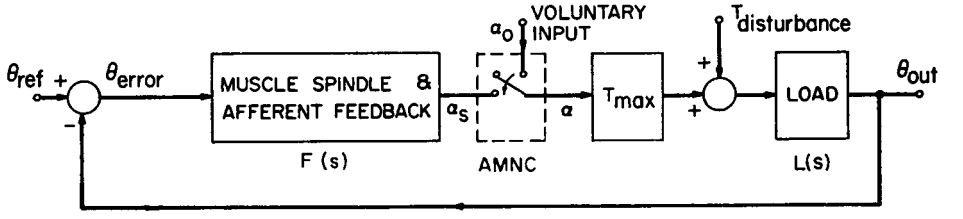

(b)

FIGURE 35 Role of alpha motor neuron "computer" (AMNC) in tracking: (*a*) original model; and (*b*) alternate version.

ACKNOWLEDGEMENTS

We wish to acknowledge partial support from the following grants and contracts: National Institutes of Health Grants NB-3055, NB-3090, MH-06175; Office of Naval Research Nonr-609(39), Nonr-1841(70); Air Force AF-33(616)-7282 and 7588, AFOSR 49(638)1313; and Army Chemical Corps DA-18-108-405-Cml-942 at the Massachusetts Institute of Technology. More recently at the Presbyterian-St. Luke's Hospital and the University of Illinois in Chicago, Ill., we have been supported in part by special grants awarded the Biomedical Engineering Department from the W. Clement and Jessie V. Stone Foundation, the Smith, Kline & French Foundation, and Public Health Research Grant FR-05477 from the General Research Support Branch, Division of Research Facilities and Resources, National Institutes of Health Grants 7-R01-MH-11907-01 PMY, 1-R01-NB-06197-01, 1-R01-NB-06487-01, and Office of Naval Research Nonr-609(39).

REFERENCES

1. BEKEY, G. A. 1962. *IRE, Trans. Human Factors Electron.* **HFE-3**:43.
2. CORTES, A. 1958. The Human Servo: Arm Control. Masters Thesis. Engineering Library, University of California. Berkeley, Calif.
3. CRAIK, K. J. W. 1947. *Brit. J. Psychol.* **38**:56, 142.
4. ELKIND, J. I. 1956. Characteristics of simple manual control systems. Tech. Rept. No. 111. Lincoln Laboratories, Mass. Inst. Technol., Lexington, Mass.
5. HALLIDAY, A. M., M. KERR, and A. ELITHSON. 1960. *J. Exptl. Psychol.* **12**:72.
6. HICK, W. E. 1948. *Quart. J. Exptl. Psychol.* **1**:36.
7. KRENDEL, E. S., and D. T. MCRUER. 1960. *J. Franklin Inst.* **169**:24.
8. LEMAY, L. P., and J. H. WESTCOTT. 1962. The simulation of human operator tracking using an intermittent model. Intern. Congr. Human Factors Electron. Long Beach, Calif.
9. LICKLIDER, J. C. R. 1960. *In* Developments in Mathematical Psychology. R. D. Luce, editor. The Free Press of Glencoe, Inc., Glencoe, Ill.
10. MCRUER, D. T. and E. S. KRENDEL. 1959. *J. Franklin Inst.* **267**:381.
11. NAVAS, F. 1963. Sampling or quantization in the human tracking system. Masters Thesis. Dept. of Electrical Engineering, Mass. Inst. Technol. Cambridge, Mass.
12. SMITH, O. J. M. 1962. *IRE, Trans. Bio-Med. Electron.* **11**:125.
13. STARK, L. 1966. Neurological Feedback Control Systems. *In* Advances in Bioengineering and Instrumentation. Chap. 4, 289. F. Alt, editor. Plenum Press, N. Y. Also HOUK, J. 1963. A Mathematical Model of the Stretch Reflex in Human Muscle Systems. Masters Thesis, Mass. Inst. Technol., Cambridge, Mass.
14. STARK, L., M. IIDA, and P. A. WILLIS. 1961. *Biophys. J.* **1**:279.
15. STARK, L., Y. OKABE, and P. A. WILLIS. 1962. *Quart. Progr. Rept.* Res. Lab. Electron. Mass. Inst. Technol. **67**:220.
16. STARK, L., Y. OKABE, P. A. WILLIS, AND H. E. RHODES. 1962. *Quart. Progr. Rept.* Res. Lab. Electron., Mass. Inst. Technol. **66**:389.
17. STARK, L., G. VOSSIUS, and L. R. YOUNG. 1962. *IRE, Trans. Human Factors Electron.* **HFE-3**:52.
18. TELFORD, C. O. 1931. *J. Exptl. Psychol.* **14**:1.
19. TUSTIN, A. 1947. *J. Inst. Elec. Engrs. (London).* **94**:190.
20. WARD, J. R. 1958. The dynamics of a human operator in a control system. Doctoral Dissertation. Dept. of Aeronautics, University of Sidney. Sidney, Australia.
21. YOUNG, L. R., and L. STARK. 1963. *IEEE, Trans. Military Electron.* **MIL-7**:113.
22. YOUNG, L. R., and L. STARK. 1963. *IEEE, Trans. Profess. Tech. Group Human Factors Electron.* Special Manual Control issue. **HFE-4**:38.